

Heavy Flavor Hadrons in Statistical Hadronization of Strangeness-rich QGP

Inga Kuznetsova and Johann Rafelski

Department of Physics, University of Arizona, Tucson, Arizona, 85721, USA

October 2, 2018

Abstract. We study b, c quark hadronization from QGP. We obtain the yields of charm and bottom flavored hadrons within the statistical hadronization model. The important novel feature of this study is that we take into account the high strangeness and entropy content of QGP, conserving strangeness and entropy yields at hadronization.

PACS. 25.75.Nq Quark deconfinement – 12.38.Mh Quark-gluon plasma in quantum chromodynamics – 25.75.-q Relativistic heavy-ion collisions – 24.10.Pa Thermal and statistical models

1 Introduction

A relatively large number of hadrons containing charmed and bottom quarks are expected to be produced in heavy ion (AA) collisions at the Large Hadrons Collider (LHC). Because of their large mass c, \bar{c}, b, \bar{b} quarks are produced predominantly in primary parton-parton collisions [1], at RHIC [2], and thus even more so at LHC. These heavy flavor quarks participate in the evolution of the dense QCD matter from the beginning. In view of the recent RHIC results it can be hoped that their momentum distribution could reach approximate thermalization within the dense QGP phase [3].

In our approach we will tacitly assume that the following evolution stages are present in heavy-ion collisions:

1. Primary partons collide producing c, b quarks;
2. A thermalized parton state within $\tau = \tau_{th} \simeq 0.25 - 1$ fm/c is formed. By the end of this stage nearly all entropy is produced.
3. The subsequent chemical equilibration: diverse thermal particle production reactions occur, allowing first the approach to chemical equilibrium by gluons g and light non-strange quarks $q = u, d$.
4. The strangeness chemical equilibration within $\tau \sim 5$ fm/c.
5. The hadronization to final state near $\tau \sim 10$ fm/c.

It is important to observe that in the presence of deconfined QGP phase heavy hadrons containing more than one heavy quark are made from heavy quarks created in different initial NN collisions. Therefore yields of these hadrons are expected to be enhanced as compared to yields seen in single NN collisions [4,5]. We note that the $B_c(b\bar{c}, \bar{b}c)$ and $J/\Psi(c\bar{c})$ and more generally all bound $c\bar{c}$ states yields were calculated before in the kinetic formation and dissociation models [4,6]. Our present work suggests that it is

important to account for the binding of heavy flavor with strangeness, an effect which depletes the eligible supply of heavy flavor quarks which could form $B_c(b\bar{c}, \bar{b}c)$ and $J/\Psi(c\bar{c})$ [7].

Enhanced production yield of multi-heavy hadrons can be considered to be an indicator of the presence of deconfined QGP phase for reasons which are analogue to those of multi-strange (anti) baryons [8]. Considering that we have little doubt that QGP is the state of matter formed in the very high energy AA interactions, the study of yields of multi-heavy hadrons is primarily explored in this work in order to falsify, or justify, features of the statistical hadronization model (SHM) employed or the model itself in the context of formation of the heavy flavor hadrons.

For example, differing from other recent studies which assume that the hadron yields after hadronization are in chemical equilibrium [5,9], we form the yields based on abundance of u, d, s quark pairs as these are available at the chemical freeze-out (particle formation) conditions in the quark-gluon phase. This approach is justified by the expectation that in a fast break-up of the QGP formed at RHIC and LHC the phase entropy and strangeness will be nearly conserved during the process of hadronization. We will investigate in quantitative terms how such chemical non-equilibrium yields, in the conditions we explore well above the chemical equilibrium abundance, influence the expected yields of single, and multi-heavy flavor hadrons.

In the order to evaluate the yields of final state hadrons we enforce conservation of entropy, and the flavor s, c, b quark pair number during phase transition or transformation. The faster the transition, the less likely it is that there is significant change in strange quark pair yield. Similarly, any entropy production is minimized when the entropy rich QGP breakup into the entropy poor HG occurs rapidly. The entropy conservation constraint fixes the final light quark yield. We assume a fast transition between

QGP and HG phases, such that all hadron yields are at the same physical conditions as in QGP breakup.

In the evaluation of heavy particle yields we form ratios involving as normalizer the total heavy flavor yield, and for yields of particles with two heavy quarks we use as normalizer the product of total yields of corresponding heavy flavors such that the results we consider is as little as possible dependent on the unknown total yield of charm and bottom at RHIC and LHC. The order of magnitude of the remaining dependence on heavy flavor yield is set by the ratio of yield of all particles with two heavy quarks to yield of particles with one heavy quark. This ratio depends on the density of heavy flavor at hadronization, $(dN_c/dy)/(dV/dy)$. The results we present for LHC are obtained for an assumed charm and bottom quark multiplicity:

$$\frac{dN_c}{dy} \equiv c = 10, \quad (1)$$

$$\frac{dN_b}{dy} \equiv b = 1. \quad (2)$$

and $dV/dy = 800 \text{ fm}^3$ at $T = 200 \text{ MeV}$. Theoretical cross sections of c and b quarks production for RHIC and LHC can be found in [10, 11]. In certain situations we will explore how variation of the baseline yields Eq. (1) and Eq. (2) impact the results. In particular among the yields of multi-heavy hadrons, this influence can be noticeable, see discussion in the end of section 6.1. We note that the number of b quarks can not change during expansion, because of large mass $m_b \gg T$. It is nearly certain that all charm in QGP at RHIC is produced in the first parton collisions, for further discussion of LHC see Ref.[12] – it appears that for all practical purposes also in the more extreme thermal conditions at LHC charm is produced in the initial parton interactions.

In order to form physical intuition about the prevailing conditions in the QGP phase at time of hadronization, we also evaluate the heavy quark chemical reference density, that is the magnitude of the chemical occupancy factor in QGP, considering the pre-established initial yields of c and b from parton collision. For this purpose we use in the deconfined QGP phase:

$$\begin{aligned} m_c &= 1.2 \text{ GeV}, \\ m_b &= 4.2 \text{ GeV} \end{aligned}$$

We also take $\lambda_i = 1, i = u, d, s$ for all light flavors, since the deviation from particle-antiparticle yield symmetry is rather small and immaterial in the present discussion.

When computing the yields of charmed (and bottom) mesons we will distinguish only strange and non-strange abundances, but not charged with non-charged (e.g. $D^- (\bar{c}d)$ with $\bar{D}^0 (\bar{c}u)$). We assume that the experimental groups reporting results, depending on which types of D-meson were observed, can infer the total yield (charged+non-charged) which we present. We treat in similar way other heavy hadrons, always focusing on the heavy and the strange flavor content and not distinguishing the light flavor content.

Our paper is organized as follows: we first introduce the elements of the SHM model we use to evaluate heavy flavor hadron yields in section 2. This allows us to discuss the relative yields of strange and non-strange heavy mesons in section 3, and we show how this result relates the value of the strangeness chemical (non-)equilibrium parameters. In this context, we also propose a multi-particle ratio as a measure of the hadronization temperature, and explore how a multi-temperature, staged, freeze-out would impact the relevant results.

Before proceeding to obtain the main results of this work we introduce the notion of conservation of entropy in section 4 and strangeness in section 5, expected to be valid in the fast hadronization process at LHC, and discuss how this impacts the SHM statistical parameters. We consider the entropy in a system with evolving strangeness in subsection 4.2 and show that the number of active degrees of freedom in a QGP is nearly constant. Another highlight is the discussion of sudden hadronization of strangeness and the associated values of hadron phase space parameters in subsection 5.4. Throughout this paper we will use explicitly and implicitly the properties of QGP fireball and hadron phase space regarding entropy and strangeness content developed in these two sections 4 and 5.

We turn to discuss the heavy flavor hadron yields for given bulk QGP constraints in section 6, where we also compare when appropriate to the strangeness and light quarks chemical equilibrium results. We begin with a study of the charm and bottom quark phase space occupancy parameters (subsection 6.1) and turn in subsection 6.2 to discussion of the yields of single heavy mesons, which we follow with discussion of yields of single heavy baryons in subsection 6.3. In last subsection 6.4 we present the expected yields of the multi-heavy hadrons, in so far these can be considered in the grand canonical approach. We conclude our work with a brief summary in section 7.

2 Statistical Hadronization Model (SHM)

The statistical hadronization model arises from the Fermi multi-particle production model [13]. Fermi considered that all hadron production matrix elements are saturated to unity. This allows the use of the Fermi golden rule with the N-particle phase space to obtain the relative particle yields. In modern language this is SHM in micro-canonical ensemble, micro-canonical implies that discrete (flavor) quantum numbers and the energy are conserved exactly.

The transition from micro-canonical to canonical, and grand-canonical ensembles simplifies the computational effort considerably [14]. This important step does not in our context introduce the hadron phase, although before the understanding of QGP this of course was the reaction picture: a highly compressed hadron gas matter evaporates particles. Today, it is the highly compressed hot quark-gluon matter that evaporates particles. In principle, there is no necessity to introduce a hadron gas phase of matter in order to use SHM to describe particle production.

On the other hand, in order to understand the physical meaning of the parameters introduced to describe hadron phase space in grand-canonical ensemble, such as temperature T , it is quite convenient to *imagine* the existence of the hadron phase which follows the QGP phase. This can be taken to the extreme, and a long lasting, chemically equilibrating phase of hadrons can be assumed, that follows in time the formation of the QGP fireball. Such a reaction picture may not agree with the fast evolving circumstance of a heavy ion collision. One should note that the study of hot hadron matter on the lattice within the realm of L-QCD involves at all times a fully equilibrated system. This will in key features differ from the non-equilibrium QGP properties accompanying the hadronization process.

The important parameters of the SHM, which control the relative yields of particles, are the particle specific fugacity factor λ and space occupancy factor γ . The fugacity is related to chemical potential $\mu = T \ln \lambda$. The occupancy γ is, nearly, the ratio of produced particles to the number of particle expected in chemical equilibrium. The actual momentum distribution is:

$$\frac{d^6 N}{d^3 p d^3 x} \equiv f(p) = \frac{g}{(2\pi)^3} \frac{1}{\gamma^{-1} \lambda^{-1} e^{E/T} \pm 1} \rightarrow \gamma \lambda e^{-E/T}, \quad (3)$$

where the Boltzmann limit of the Fermi ‘(+)’ and Bose ‘(-)’ distributions is indicated, g is the degeneracy factor, T is the temperature and $E = E(p)$ is the energy.

The fugacity λ is associated with a conserved quantum number, such as net-baryon number, net-strangeness, heavy flavor. Thus antiparticles have inverse value of λ , and λ evolution during the reaction process is related to the changes in densities due to dynamics such as expansion. γ is the same for particles and antiparticles. Its value changes as a function of time even if the system does not expand, for it describes buildup of the particular particle species. For this reason γ is changes rapidly during the reaction, while λ is more constant. Thus it is γ which carries the information about the time history of the reaction and the precise condition of particle production referred to as chemical freeze-out.

The number of particles of type ‘ i ’ with mass m_i per unit of rapidity is in our approach given by:

$$\frac{dN_i}{dy} = \gamma_i n_i^{\text{eq}} \frac{dV}{dy}. \quad (4)$$

Here dV/dy is system volume associated with the unit of rapidity, and n_i^{eq} is a Boltzmann particle density in chemical equilibrium:

$$\begin{aligned} n_i^{\text{eq}} &= g_i \int \frac{d^3 p}{(2\pi)^3} \lambda_i \exp(-\sqrt{p^2 + m_i^2}/T) \\ &= \lambda_i \frac{T^3}{2\pi^2} g_i W(m_i/T), \end{aligned} \quad (5)$$

and

$$W(x) = x^2 K_2(x) \rightarrow 2 \text{ for } x \rightarrow 0. \quad (6)$$

Both, $m_i c^2 \rightarrow m_i$, and $kT \rightarrow T$, are measured in energy units when $\hbar, c, k \rightarrow 1$.

For the case of heavy flavors $m \gg T$, the dominant contribution to the Boltzmann integral Eq. (5) arises from $p \simeq \sqrt{2mT}$, we do not probe the tails of the momentum distribution. Thus even when the momentum distribution is not well thermalized, the yield of heavy flavor hadrons can be described in term of the thermal yields, Eq.(4), where:

$$\begin{aligned} n_i^{\text{eq}} &= \frac{g_i T^3}{2\pi^2} \lambda_i \sqrt{\frac{\pi m_i^3}{2T^3}} \exp(-m_i/T) \times \\ &\times \left(1 + \frac{15T}{8m_i} + \frac{105}{128} \left(\frac{T}{m_i} \right)^2 \dots \right). \end{aligned} \quad (7)$$

Often one can use the first term alone for heavy flavor hadrons, since $T/m \ll 1$, however the asymptotic series in Eq. (7) has limited validity. Our computations are all based on CERN recursive subroutine evaluation of the Bessel K_2 functions.

We use occupancy factors γ_i^{Q} and γ_i^{H} for QGP and hadronic gas phase respectively, tracking every quark flavor ($i = q, s, b, c$). We assume that in the QGP phase the light quarks and gluons are adjusting fast to the ambient conditions, and thus are in chemical equilibrium with $\gamma_{q,G}^{\text{Q}} \rightarrow 1$. For heavy, and strange flavor, the value of γ_i^{Q} at hadronization condition is given by the number of particles present, generated by prior kinetic processes, see Eq. (4).

The yields of different quark flavors originate in different physical processes, such as production in initial collisions for c, b, s , and for s also production in thermal plasma processes. In general we thus cannot expect that $\gamma_{c,b}^{\text{Q}}$ will be near unity at hadronization. However, the thermal strangeness production process $GG \rightarrow s\bar{s}$ can nearly chemically equilibrate strangeness flavor in plasma formed at RHIC and/or LHC [12], and we will always consider, among other cases the limit $\gamma_s^{\text{Q}} \rightarrow 1$ prior to hadronization.

The yields of all hadrons after hadronization are also given by Eq. (4), which helps us to obtain γ_i^{H} for hadrons. In general, the evaluation of hadron chemical parameters presents a more complicated case since they are composed from those of valance quarks in the hadron (three quarks, or a quark and anti quark). Therefore, in the coalescence picture, the phase space occupancy γ^{H} of hadrons will be the product of γ^{H} 's for each constituent quark. For example for the charmed meson D ($c\bar{q}$)

$$\gamma_D^{\text{H}} = \gamma_c^{\text{H}} \gamma_q^{\text{H}}. \quad (8)$$

To evaluate yields of final state hadrons we enforce conservation of entropy, and the flavor s, c, b quark pair number during phase transition or transformation. The faster the transition, the less likely is that there is significant change in strange quark pair yield. Similarly, any entropy production is minimized when the entropy rich QGP breakup into the entropy poor HG occurs rapidly. The entropy conservation constraint fixes the final light quark yield. We assume a fast transition between QGP and HG phases, such that all hadron yields are at the same physical conditions as in QGP breakup.

Assuming that in the hadronization process the number of b , c , s quark pairs doesn't change, the three unknown γ_s^H , γ_c^H , γ_b^H can be determined from their values in the QGP phase, γ_s^Q , γ_c^Q , γ_b^Q (or dN_i^Q/dy) and the three flavor conservation equations,

$$\frac{dN_i^H}{dy} = \frac{dN_i^Q}{dy} = \frac{dN_i}{dy}, \quad i = s, c, b. \quad (9)$$

In order to conserve entropy:

$$\frac{dS^H}{dy} = \frac{dS^Q}{dy} = \frac{dS}{dy}, \quad (10)$$

a value $\gamma_q^H \neq 1$ is nearly always required when in the QGP phase $\gamma_{q,G}^Q = 1$. This implies that yields of hadrons with light quark content are, in general, not in chemical equilibrium, unless there is some extraordinary circumstance allowing a prolonged period of time in which hadron reactions can occur after hadronization. Chemical non-equilibrium thus will influence the yields of heavy flavored particles in final state as we shall discuss in this work.

As noted at the beginning of this section, the use of the hadron phase space (denoted by H above) does not imply the presence of a real physical 'hadron matter' phase: the SHM particle yields will be attained solely on the basis of availability of this phase space as noted at the beginning of this section. Another way to argue this is to imagine a pot of quark matter with hadrons evaporating. Which kind of hadron emerges and at which momentum is entirely determined by the access to the phase space, and there are only free-streaming particles in the final state.

Thinking in these terms, one can imagine that especially for heavy quark hadrons some particles are preformed in the deconfined plasma, and thus the heavy hadron yields may be based on a value of temperature which is higher than the global value expected for other hadrons. For this reason we will study in this work a range $140 < T < 260$ MeV and also consider sensitivity to this type of two-temperature chemical freeze-out of certain heavy hadron yield ratios.

3 Relative charmed hadron yields

3.1 Determination of γ_s/γ_q

We have seen considering s/S and also s and S individually across the phase limit that in general one would expect chemical non-equilibrium in hadronization of chemically equilibrated QGP. We first show that this result matters for the relative charm meson yield ratio D_s/D , where $D_s(c\bar{s})$ comprises all mesons of type $(c\bar{s})$ which are listed in the bottom section of table 1, and $D(c\bar{q})$ comprise yields of all $(c\bar{q})$ states listed in the top section of table 1. This ratio is formed based on the assumption that on the time scale of strong interactions the family of strange-charmed mesons can be distinguished from the family non-strange charmed mesons.

Table 1. Open charm, and bottom, hadron states we considered. States in parenthesis either need confirmation or have not been observed experimentally, in which case we follow the values of Refs. [15, 30]. We implemented charm-bottom symmetry required for certain observables. Top section: D , B mesons, bottom section: D_s , B_s -mesons

hadron	M[GeV]	Q:c,b	hadron	M[GeV]	g
$D^0(0^-)$	1.8646	$Q\bar{u}$	$B^0(0^-)$	5.279	1
$D^+(0^-)$	1.8694	$Q\bar{d}$	$B^+(0^-)$	5.279	1
$D^{*0}(1^-)$	2.0067	$Q\bar{u}$	$B^{*0}(1^-)$	5.325	3
$D^{*+}(1^-)$	2.0100	$Q\bar{d}$	$B^{*+}(1^-)$	5.325	3
$D^0(0^+)$	2.352	$Q\bar{u}$	$B^0(0^+)$	5.697	1
$D^+(0^+)$	2.403	$Q\bar{d}$	$B^+(0^+)$	5.697	1
$D_1^{*0}(1^+)$	2.4222	$Q\bar{u}$	$B_1^{*0}(1^+)$	5.720	3
$D_1^{*+}(1^+)$	2.4222	$Q\bar{d}$	$B_1^{*+}(1^+)$	5.720	3
$D_2^{*0}(2^+)$	2.4589	$Q\bar{u}$	$B_2^{*0}(2^+)$	(5.730)	5
$D_2^{*+}(2^+)$	2.4590	$Q\bar{d}$	$B_2^{*+}(2^+)$	(5.730)	5
$D_s^+(0^-)$	1.9868	$Q\bar{s}$	$B_s^0(0^-)$	5.3696	1
$D_s^{*+}(1^-)$	2.112	$Q\bar{s}$	$B_s^{*0}(1^-)$	5.416	3
$D_{sJ}^{*+}(0^+)$	2.317	$Q\bar{s}$	$B_{sJ}^{*0}(0^+)$	(5.716)	1
$D_{sJ}^{*+}(1^+)$	2.4593	$Q\bar{s}$	$B_{sJ}^{*0}(1^+)$	(5.760)	3
$D_{sJ}^{*+}(2^+)$	2.573	$Q\bar{s}$	$B_{sJ}^{*0}(2^+)$	(5.850)	5

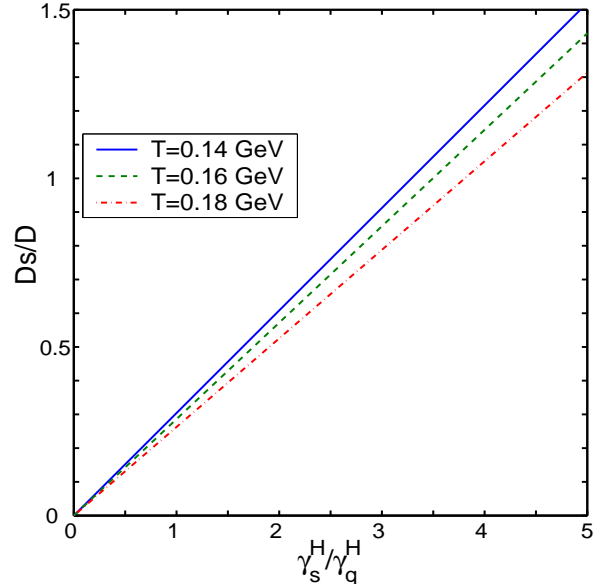


Fig. 1. (Color on line) D/D_s ratio as a function of γ_s^H/γ_q^H for $T = 140$ MeV (blue, solid line), $T = 160$ MeV (green, dashed line) and $T = 180$ MeV (red, dash-dot line).

The yield ratio D_s/D calculated using Eq. (4) and Eq. (5) is shown in figure 1. Using Eq. (7) we see that this ratio is proportional to γ_s^H/γ_q^H and weakly dependent on T :

$$\frac{D_s}{D} \approx \frac{\gamma_s^H}{\gamma_q^H} \frac{\sum_i g_{D_{si}} m_{D_{si}}^{3/2} \exp(-m_{D_{si}}/T)}{\sum_i g_{D_i} m_{D_i}^{3/2} \exp(-m_{D_i}/T)} = f(T) \frac{\gamma_s^H}{\gamma_q^H}. \quad (11)$$

A deviation of γ_s/γ_q from unity in the range we will see in section 5.4 leads to a noticeable difference in the ratio D_s/D . We show in figure 1 results for $T = 140, 160, 180$ MeV. In this T -domain, the effect due to $\gamma_s^H/\gamma_q^{rmH} \neq 1$ is

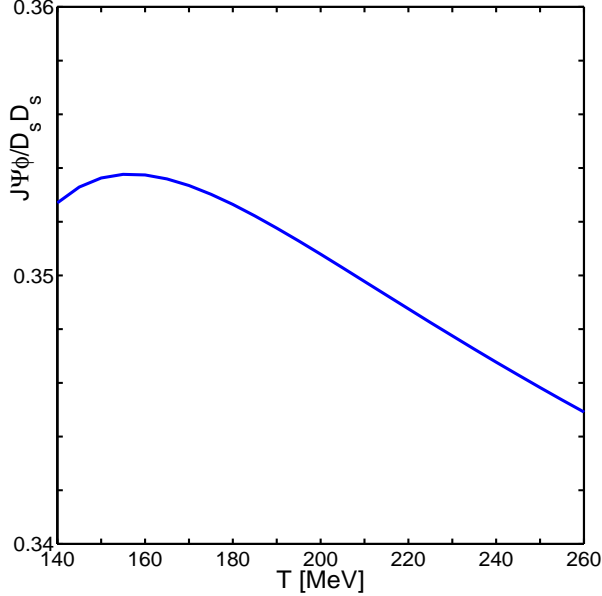


Fig. 2. (Color on line) $J/\Psi \phi / D_s \overline{D}_s$ ratio as a function of hadronization temperature T .

the dominant contribution to the variation of this relative yield.

3.2 Check of statistical hadronization model

We next construct a heavy flavor particle ratio that depends on hadronization temperature only. To cancel the fugacities and the volume we consider the ratio $J/\Psi \phi / D_s \overline{D}_s$ in figure 2. Here J/Ψ yield includes the yield of $(c\bar{c})$ mesons decaying into the J/Ψ . All phase space occupancies cancel since $J/\Psi \propto \gamma_c^{H^2}$, $\phi \propto \gamma_s^{H^2}$, $D_s \propto \gamma_c^H \gamma_s^H$ and similarly $\overline{D}_s \propto \gamma_c^H \gamma_s^H$. When using here the particle $D_s(c\bar{s})$ and antiparticle $\overline{D}_s(c\bar{s})$ any chemical potentials present are canceled as well. However, for the LHC and even RHIC environments this refinement is immaterial.

This ratio $J/\Psi \phi / D_s \overline{D}_s$, turns out to be practically constant, within a rather wide range of hadronization temperature T , see figure 2. The temperature range we study $140 < T < 280$ MeV allows us to consider an early freeze-out of different hadrons. To be sure of the temperature independence of $J/\Psi \phi / D_s \overline{D}_s$ we next consider the possibility that hadronization temperature T of charmed hadrons is higher than hadronization temperature T_0 of ϕ . We study this question by exploring the sensitivity of the ratio $J/\Psi \phi / D_s \overline{D}_s$ to the two temperature freeze-out in figure 3, see bottom three lines for $T_0 = 180, 160, 140$ MeV with γ_q from condition $S^Q = S^H$, see figure 6. If charmed hadrons hadronize later, $T > T_0$, and $T - T_0 < 60$ the change in $J/\Psi \phi / D_s \overline{D}_s$ ratio is small (about 20%). If this were to be measured as experimental result,

$$\frac{J/\Psi \phi}{D_s \overline{D}_s} \simeq 0.35, \quad (12)$$

one could not but conclude that all particles involved are formed by mechanism of statistical hadronization.

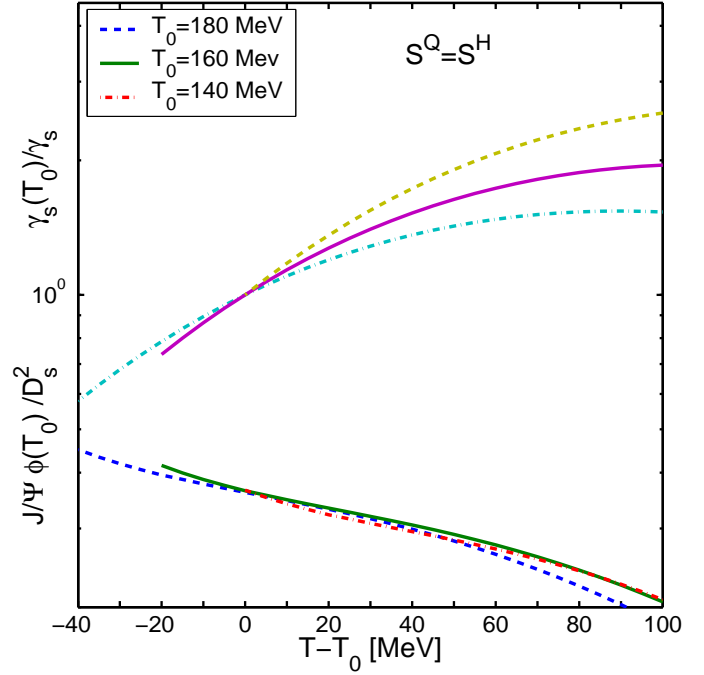


Fig. 3. (Color on line) $J/\Psi \phi(T_0) / D_s \overline{D}_s$ ratio is evaluated at two temperatures, T for heavy flavor hadrons, and T_0 for ϕ as a function of $T - T_0$, with three values of $T_0 = 140, 160, 180$ MeV is considered with $S^H = S^Q$.

This interesting result can be understood, considering the behavior of the $\gamma_s^H(T_0) / \gamma_s^H(T)$ ratio, which increases rapidly with increasing $T - T_0$ (see the top three lines in figure 3). This ratio almost compensates the change in ϕ -yield, an effect we already encountered in the context of the results we show below in figure 9. For large $T - T_0$ the ratio $J/\Psi \phi / D_s \overline{D}_s$ begins to decrease more rapidly because γ_s increases for $S^H = S^Q$, see figure (6).

4 Entropy in Hadronization

4.1 Entropy in QGP fireball

The entropy content is seen in the final state multiplicity of particles produced after hadronization. More specifically, there is a relation between entropy and particles multiplicities, once we note that the entropy per particle in a gas is:

$$\frac{S_B}{N} = 3.61, \quad \frac{S_{cl}}{N} = 4, \quad \frac{S_F}{N} = 4.2, \quad (13)$$

for massless Bose, classical (Boltzmann) and Fermi gases, respectively. Effectively, for QGP with u, s, d, G degrees of freedom, $S^Q / N^Q \sim 4$ is applicable for large range of masses. Thus:

$$\frac{dS^Q}{dy} \approx 4 \frac{dN^Q}{dy}. \quad (14)$$

This in turn means that final state particle multiplicity provides us with information about the primary entropy content generated in the initial state of the QGP phase.

It is today generally believed that there is entropy conserving hydrodynamic expansion of the QGP liquid. Entropy is conserved in the fireball, and the conservation of entropy density σ flow is expressed by:

$$\frac{\partial_\mu(\sigma u^\mu)}{\partial x^\mu} = 0, \quad (15)$$

where u^μ is local four velocity vector. A special case of interest is the so-called Bjørken scenario [16] for which Eq. (15) can be solved exactly assuming as initial condition scaling of the physical properties as a function of rapidity. This implies that there is no preferred frame of reference, a situation expected in very high energy collisions. Even if highly idealized, this simple reaction picture allows a good estimate of many physical features. Of relevance here is that the exact solution of hydrodynamics in (1+1) dimensions implies

$$\frac{dS}{dy} = \text{Const.} \quad (16)$$

Thus entropy S is not only conserved globally in the hydrodynamic expansion, but also per unit of rapidity. Though we have (1+3) expansion, Eq.(16) holds as long as there is, in rapidity, a flat plateau of particles yields. Namely, each of the domains of rapidity is equivalent, excluding the projectile-target domains. However, at RHIC and LHC energies these are causally disconnected from the central rapidity bin, where we study the evolution of heavy flavor. The entropy we observe in the final hadron state has been to a large extent produced after the heavy flavor is produced, during the initial parton thermalization phase, but before strangeness has been produced. In order to model production of hadrons for different chemical freeze-out scenarios of the same reaction, we need to relate the entropy content, temperature and volume of the QGP domain. We consider for a u, d, G -chemically equilibrated QGP, and allowing for partial chemical equilibration of strangeness, the entropy content.

The entropy density σ can be obtained from the equation

$$\sigma \equiv \frac{S}{V} = -\frac{1}{V} \frac{dF_Q}{dT}, \quad (17)$$

where the thermodynamic potential is:

$$F_Q(T, \lambda_q, V) = -T \ln Z(QT, \lambda_q, V)_Q. \quad (18)$$

Inside QGP the partition function is a product of partition function of gluons Z_g , light quarks Z_q and strange quarks Z_s , hence:

$$\ln Z = \ln Z_g + \ln Z_q + \ln Z_s; \quad (19)$$

where for massless particles with $\lambda_q = 1$

$$\ln Z_g = \frac{g_g \pi^2}{90} VT^3, \quad (20)$$

$$\ln Z_q = \frac{7}{4} \frac{g_q \pi^2}{90} VT^3. \quad (21)$$

Here g_g is degeneracy factor for gluons and g_q is degeneracy factor for quarks. The factor $7/4 = 2 \cdot 7/8$ accounts for the difference in statistics and presence of both quarks and antiquarks. The number of degrees of freedom of quarks and gluons is influenced by strongly interactions, characterized by strong coupling constant α_s :

$$g_g = 2_s 8_c \left(1 - \frac{15}{4\pi} \alpha_s + \dots\right); \quad (22)$$

$$g_q = 2_s 3_c 2_f \left(1 - \frac{50}{21\pi} \alpha_s + \dots\right). \quad (23)$$

The case of strange quarks is somewhat more complicated, since we have to consider the mass, the degree of chemical equilibration, and guess-estimate the strength of QCD perturbative interactions. We have in Boltzman approximation:

$$\ln Z_s = 2_{p/a} \frac{g_s}{\pi^2} VT^3, \quad (24)$$

$$g_s = 2_s 3_c \gamma_s^Q 0.5W(m_s/T) \left(1 - k \frac{\alpha_s}{\pi}\right). \quad (25)$$

$W(m/T)$ is function seen in Eq. (6). We allow both for strange and antistrange quarks, factor $2_{p/a}$ (which is for massless fermions $2 \cdot 7/8 = 7/4$). k at this point is a temperature dependent parameter. Even in the lowest order perturbation theory it has not been evaluated for massive quarks at finite temperature. We know that for massless quarks $k \simeq 2$. Considering expansion in m/T , for large masses the correction reverses sign [17], which result supports the reduction in value of k for $m \simeq T$. We will use here the value $k = 1$ [12].

4.2 Number of degrees of freedom in QGP

The entropy density following from Eq. (17) is:

$$\sigma = \frac{4\pi^2}{90} (g_g + \frac{7}{4} g_q) T^3 + \frac{4}{\pi^2} 2_{p/a} g_s T^3 + \frac{\mathcal{A}}{T}. \quad (26)$$

For strange quarks in the second term in Eq. (26) we set the entropy per strange quarks to 4 units. In choosing $S_s/N_s = 4$ irrespective of the effect of interaction and mass value m_s/T we are minimizing the influence of unknown QCD interaction effect.

The last term in Eq. (26) comes from differentiation of the strong coupling constant α_s in the partition function with respect to T , see Eq.(17). Up to two loops in the β -function of the renormalization group the correction term is [18]:

$$\mathcal{A} = (b_0 \alpha_s^2 + b_1 \alpha_s^3) \left[\frac{2\pi}{3} T^4 + \frac{n_f 5\pi}{18} T^4 \right] \quad (27)$$

with n_f being the number of active fermions in the quark loop, $n_f \simeq 2.5$, and

$$b_0 = \frac{1}{2\pi} \left(11 - \frac{2}{3} n_f\right), \quad b_1 = \frac{1}{4\pi^2} \left(51 - \frac{19}{3} n_f\right). \quad (28)$$

For the strong coupling constant α_s we use

$$\alpha_s(T) \simeq \frac{\alpha_s(T_c)}{1 + C \ln(T/T_c)}, \quad C = 0.760 \pm 0.002, \quad (29)$$

where $T_c = 0.16$ GeV. This expression arises from renormalization group running of $\alpha_s(\mu)$, the energy scale at $\mu = 2\pi T$, and the value $\alpha_s(M_Z) = 0.118$. A much more sophisticated study of the entropy in the QGP phase is possible [19], what we use here is an effective model which agrees with the lattice data [20].

Eq. (26) suggests that we introduce an effective degeneracy of the QGP based on the expression we use for entropy:

$$g_{\text{eff}}^Q(T) = g_g(T) + \frac{7}{4}g_q(T) + 2g_s \frac{90}{\pi^4} + \frac{\mathcal{A}}{T^4} \frac{90}{4\pi^2}. \quad (30)$$

Which allows us to write:

$$\sigma = \frac{4\pi^2}{90} g_{\text{eff}}^Q T^3, \quad (31)$$

and

$$\frac{dS}{dy} = \frac{4\pi^2}{90} g_{\text{eff}}^Q T^3 \frac{dV}{dy} \simeq \text{Const.} \quad (32)$$

We show the QGP degeneracy in figure 4, as a function of $T \in [140, 260]$ MeV, top frame for fixed $s/S = 0, 0.03, 0.04$ (from bottom to top), and in the bottom frame for the strangeness chemical equilibrium, $\gamma_s = 1$ (dashed) and approach to chemical equilibrium cases (solid). When we fix the specific strangeness content s/S in the plasma comparing different temperatures we find that in all cases g_{eff}^Q increases with T . For $s/S = 0$ we have a 2-flavor system (dotted line, red) and the effective number of degrees of freedom g_{eff}^Q varies between 22 and 26. The solid line with dots (green) is for $s/S = 0.03$, and the dot-dashed line (blue) gives the result for $s/S = 0.04$.

In the bottom panel of figure 4 we note that like for 2 flavors, case ($s=0$), for the 2+1-flavor system ($\gamma_s = 1$) g_{eff}^Q increases with T (dashed line, black). g_{eff}^Q varies between 30 and 35.5. The thin dashed lines indicate the range of uncertainty due to mass of the strange quark, which in this calculation is fixed with upper curve corresponding to $m_s = 90$ MeV, and lower one $m_s = 160$ MeV. The expected decrease in value of m_s with T will thus have the effect to steepen the rise in the degrees of freedom with T .

We now explore in a QGP phase the effect of an increasing strangeness fugacity with decreasing temperature. This study is a bit different from the rest of this paper, where we consider for comparison purposes hadronization for a range of temperatures but at a *fixed* value of s/S . A variable $\gamma_s^Q(T)$ implies a more sophisticated, and thus more model dependent picture of plasma evolution. However, this offers us an important insight about g_{eff}^Q .

We consider the function:

$$\gamma_s^Q = \frac{300 - T[\text{MeV}]}{160}. \quad (33)$$

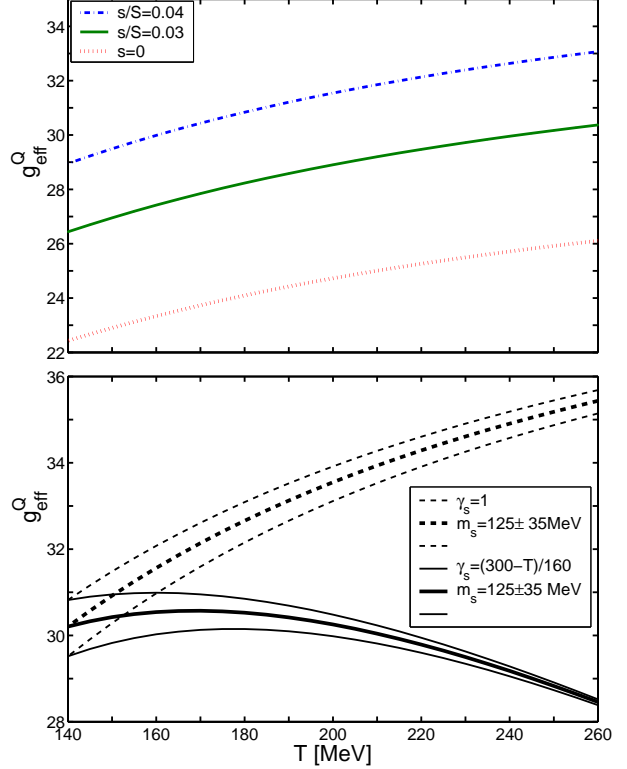


Fig. 4. (color on-line) The Stefan-Boltzmann degrees of freedom g_{eff}^Q based on entropy content of QGP, as function of temperature T . Upper frame: fixed s/S , the solid line with dots (green) is for a system with fixed strangeness per entropy $s/S = 0.03$, while dot-dashed (blue) line is for $s/S = 0.04$. The dotted (red) line is for 2-flavor QCD $s/S = 0$ (u, d, G only); The bottom frame shows dashed (black) line 2+1-flavor QCD with $m_s = 125 \pm 35$ MeV (chemically equilibrated u, d, s, G system). The (thick, thin) solid lines are for QGP in which strangeness contents is increasing as a function of temperature, see text.

This is consistent with the kinetic computation of strangeness production [12]. At $T = 140$ MeV we have chemical equilibrium in the QGP phase, while and at the temperature $T = 260$ MeV we have $\gamma_s = 0.25$. The result for g_{eff}^Q is shown as a thick (black) line in figure 4, with the range showing strange quark mass range $m_s = 125 \pm 35$ MeV. We see that in a wide range of temperatures we have $29.5 < g_{\text{eff}}^Q < 30.5$.

The lesson is that with the growth of γ_s^Q with decreasing T the entropy of the QGP is well described by a constant value $g_{\text{eff}}^Q = 30 \pm 0.5$. Since the entropy is (nearly) conserved and g_{eff}^Q is (nearly) constant, Eq. (32) implies that we can scale the system properties using the constraint $T^3 dV/dy = \text{Const}$. We stress again that these results arises in a realistic QGP with $2 + \gamma_s^Q$ -flavors, but are model dependent and of course rely on the lattice motivated description of the behavior of QGP properties. On the other hand it is not surprising that the rise of strangeness chemical saturation with decreasing temperature compensates the ‘freezing’ of the q, G -degrees of freedom with decreasing temperature.

Table 2. Reference values of volume, temperature, entropy, particle multiplicity

dV/dy [fm^3]	T [MeV]	dS^Q/dy	dN^Q/dy	dN^H/dy
800	200	10,970	2,700	5,000
2300	140	10,890	2,700	4,500

4.3 Entropy content and chemical (non-)equilibrium

We use as a reference a QGP state with $dV/dy = 800 \text{ fm}^3$ at $T = 200 \text{ MeV}$, see table 2. We find from Eq. (14) the Q and H phase particle multiplicity. The hadron multiplicity stated is what results after secondary resonance decays. The total hadron multiplicity after hadronization and resonance decays was calculated using on-line SHARE 2.1 [21]. If a greater (smaller) yield of final state hadrons is observed at LHC, the value of dV/dy need to be revised up (down). In general expansion before hadronization will not alter dS/dy . We can expect that as T decreases, $V^{1/3}$ increases. Stretching the validity of Eq. (32) to low temperature $T = 140 \text{ MeV}$, we see the result in the second line of table 2.

For QGP, in general the entropy content is higher than in a comparable volume of chemically equilibrated hadron matter, because of the liberation of color degrees of freedom in the color-deconfined phase. The total entropy has to be conserved during transition between QGP and HG phases, and thus after hadronization, the excess of entropy is observed in excess particle multiplicity, which can be interpreted as a signature of deconfinement [22, 23]. The dynamics of the transformation of QGP into HG determines how this additional entropy manifests itself.

The comparison of entropy in both phases is temperature dependent but in the domain of interest i.e. $140 < T < 180 \text{ MeV}$ the entropy density follows:

$$\sigma^Q \gtrsim 3\sigma^H. \quad (34)$$

Since the total entropy S is conserved or slightly increases, in the hadronization process some key parameter must grow in the hadronization process. There are two options: a) either the volume changes:

$$3V^H \gtrsim V^Q; \quad (35)$$

or

b) the phase occupancies change, and since $n_i \propto \gamma_i^{2,3}$, $i = q, s$ in hadron phase

$$\gamma_q^H \simeq \sqrt{3}, \quad \gamma_s^H/\gamma_q^H \gtrsim 1. \quad (36)$$

In a slow, on hadronic time scale, transition, such as is the case in the early Universe, we can expect that case a) prevails. In high energy heavy ion collisions, there is no evidence in the experimental results for the long co-existence of hadron and quark phases which is required for volume growth. Consequently, we have $V^H \sim V^Q$ and a large value of γ_q^H is required to conserve entropy. The value of γ_q^H is restricted by

$$\gamma_q^{\text{cr}} \cong \exp(m_\pi^0/2T). \quad (37)$$

This value γ_q^{cr} is near to maximum allowed value, which arises at condition of Bose-Einstein condensation of pions. We will discuss quantitative results for γ_q^H (and γ_s^H) below in subsection 5.4.

5 Strangeness in Hadronization

5.1 Abundance in QGP and HG

The efficiency of strangeness production depends on energy and collision centrality of heavy ions collisions. The increase, with value of centrality (participant number), of per-baryon specific strangeness yield indicates presents of strangeness production mechanism acting beyond the first collision dynamics. The thermal gluon fusion to strangeness can explain this behavior [8], and a model of the flow dynamics at RHIC and LHC suggests that the QGP approaches chemical equilibrium but also can exceed it at time of hadronization [12].

The strangeness yield in chemically equilibrated QGP is usually described as an ideal Boltzman gas. However, a significant correction is expected due to perturbative QCD effects. We implement this correction based on comments below Eq. (25). We use here the expression:

$$\frac{dN_s^Q}{dy} = \gamma_s^Q \left(1 - \frac{\alpha_s}{\pi}\right) n_s^{\text{eq}} \frac{dV}{dy}. \quad (38)$$

with the Boltzman limit density Eq. (5), and mass $m_s = 125 \text{ MeV}$, $g_s = 6$, $\lambda_s = 1$. The QCD correction corresponds to discussion of entropy in subsection 4.1

We obtain strange quarks phase space occupancy γ_s^H as a function of temperature from condition of equality of the number of strange quark and antiquark pairs in QGP and HG. Specifically, in the sudden QGP hadronization, quarks recombine and we expect that the strangeness content does not significantly change. For heavier flavors across the phase boundary this condition Eq. (9) is very well satisfied, for strangeness the fragmentation effect adds somewhat to the yield,

$$\frac{dN_s^H}{dy} \gtrsim \frac{dN_s^Q}{dy}. \quad (39)$$

Using the equality of yields we underestimate slightly the value of strangeness occupancy that results. We recall that we also conserve entropy Eq. (10) which like strangeness can in principle grow in hadronization,

$$\left. \frac{s}{S} \right|_H \gtrsim \left. \frac{s}{S} \right|_Q. \quad (40)$$

using Eq. (10) we underestimate the value of γ_q^{H2} .

Counting all strange particles, the number of pairs is:

$$\begin{aligned} \frac{dN_s^H}{dy} = \frac{dV}{dy} & \left\{ \gamma_s^H (\gamma_q^H n_K^{\text{eq}} + \gamma_q^{H2} n_Y^{\text{eq}}) \right. \\ & + \gamma_s^{H2} (2\gamma_q^H n_\Xi^{\text{eq}} + n_\phi^{\text{eq}} + P_s n_\eta^{\text{eq}}) \\ & \left. + 3\gamma_s^{H3} n_\Omega^{\text{eq}} \right\}, \end{aligned} \quad (41)$$

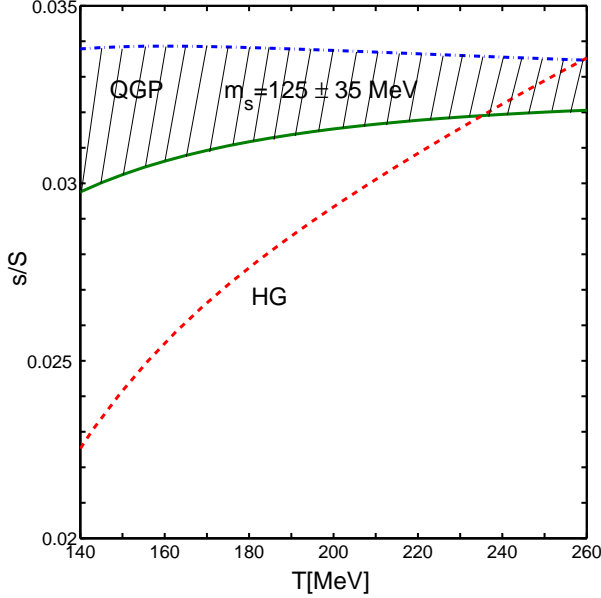


Fig. 5. (Color on line) Strangeness to entropy ratio s/S as function of temperature T , for the QGP (green, solid line for $m_s = 160$ MeV, blue dash-dot line for $m_s = 90$ MeV) with $k = 1$, see Eq. (38); and for HG (light blue, dashed line) phases for $\gamma_q = \gamma_s = \lambda_q = \lambda_s = 1$ in both phases.

where n_i^{eq} are densities of strange hadrons (mesons and baryons) calculated using Eq. (4) in chemical equilibrium. P_s is the strangeness content of the η . The way we count hadrons is to follow strangeness content, for example $n_K^{\text{eq}} = n_{K^+}^{\text{eq}} + n_{K^0}^{\text{eq}} = n_{K^-}^{\text{eq}} + n_{\bar{K}^0}^{\text{eq}}$. We impose in our calculations $\bar{s} = s$. The pattern of this calculation follows an established approach, SHARE 2.1 [21] was used in detailed evaluation.

5.2 Strangeness per entropy s/S

Considering that both strangeness, and entropy, are conserved in the hadronization process, a convenient variable to consider as fixed in the hadronization process, is the ratio of these conserved quantities s/S . In chemical equilibrium we expect that in general such a ratio must be different for different phases of matter from which particles are produced [24, 25, 12].

We compare QGP and HG specific per entropy strangeness content in figure 5. We show as function of temperature T the s/S ratios for chemically equilibrated QGP and HG phase. For the QGP the entropy S in QGP is calculated as described in section 4, and we use $k = 1$ in Eq. (38). The shaded area shows the range of masses of strange quarks, considered, results for $m_s = 90$ MeV (upper (blue) dash-dotted line) and $m_s = 160$ MeV ((green) solid line) form the boundaries. The central QGP value is at about $s/S = 0.032$.

The short-dashed (light blue) line shows the hadron phase s/S value found using SHARE 2.1. For HG near to usual range of hadronization temperature $T \simeq 160$ MeV we find $s/S \simeq 0.025$. In general formation of QGP implies

and increase by 30% in s/S . Both HG and QGP phases have a similar specific strangeness content at $T = 240$ – 260 MeV, however it is not believed that a HG at such high temperature would be a stable form of matter. This HG to QGP dissociation, or QGP hadronization depends on the degree of strangeness equilibration in plasma [29], and other dynamical factors.

In the QGP the value of s/S for the range of realistic hadronization temperature $140 < T < 180$ MeV is in general larger than in HG. This implies that generally, the abundance of strange hadrons produced in hadronization over saturates the strange hadron phase space, if QGP state had reached (near) chemical equilibrium. Moreover, since we are considering the ratio s/S and find in QGP a value greater than in HG, for chemical equilibrium in QGP the hadronization process will lead to $\gamma_s^{\text{H}}/\gamma_q^{\text{H}} > 1$.

One can wonder if we have not overlooked some dynamical or microscopic effect which could adjust the value of s/S implied by QGP to the value expected in HG. First we note that the fast growth of the volume V cannot change s/S . Moreover, any additional strangeness production in hadronization would enhance the over-abundance recorded in the resulting HG. Only a highly significant entropy production at fixed strangeness yield in the hadronization process could bring the QGP s/S ratio down, masking strangeness over-saturation. A mechanism for such entropy production in hadronization is unknown, and moreover, this would further entail an unexpected and high hadron multiplicity excess.

One could of course argue that the perturbative QCD properties in the QGP are meaningless, the entropy in QGP is much higher at given temperature. However, the properties of QGP have been checked against the lattice results, and the use of lowest order expressions is justified in these terms [20]. Moreover, the value of s/S is established way before hadronization.

5.3 Wróblewski ratio W_s

At this point it is appropriate to look at another observable proposed to study strangeness yield, the Wróblewski ratio [26]:

$$W_s \equiv \frac{2\langle \bar{s}s \rangle}{\langle \bar{u}u \rangle + \langle \bar{d}d \rangle}. \quad (42)$$

W_s compares the number of newly produced strange quarks to the produced number of light quarks. In an equilibrated deconfined phase W_s compares the number of active strange quark degrees of freedom to the number of light quark degrees of freedom.

The ratio s/S compares the strange quark degrees of freedom to all degrees of freedom available in QGP. Therefore as function of T the ratios s/S and W_s can behave differently: Considering the limit $T \rightarrow T_c$ a constant s/S indicates that the reduction of s -degrees of freedom goes hand in hand with the ‘freezing’ of gluon degrees of freedom, which precedes the ‘freezing’ of light quarks. This also implies that for $T \rightarrow T_c$ in general W_s diminishes.

The magnitude of m_s , the strange quark mass decisively enters the limit $T \rightarrow T_c$.

For $T \gg T_c$ the ratio W_s can be evaluated comparing the rates of production of light and strange quarks, using the fluctuation-dissipation theorem [27], which allows to relate rate of quark production to quark susceptibilities χ_i (see Eqs. (11) and (12) in [27]):

$$W_s \simeq R_\chi = \frac{2\chi_s}{\chi_u + \chi_d}. \quad (43)$$

An evaluation of R_χ as function of temperature in lattice QCD has been achieved [28]. For $T \simeq 2.5T_c$ the result obtained, $W_s \rightarrow R_\chi \simeq 0.8$, is in agreement with the expectation for equilibrium QGP with nearly free quarks, with mass of strangeness having a small but noticeable significance. With decreasing T , the ratio $R_\chi \rightarrow 0.3$ for $m_s = T_c$. However, this value of m_s is too large, the physical value should be nearly half as large, which would result in a greater R_χ . Moreover, for $T \rightarrow T_c$ the relationship of W_s to R_χ , Eq. (43) is in question in that the greatly reduced rate of production of strangeness may not be satisfying the conditions required in Ref. [27].

Comparing the observables s/S and W_s we note that the experimental measurement requires in both cases a detailed analysis of all particles produced. At lower reaction energies there is additional complication in evaluation of W_s due to the need to subtract the effect of quarks brought into the reaction region. Turning to the theoretical computation of s/S and W_s we note that the thermal lattice QCD evaluation of s/S is possible without any approximation, even if the actual computation of entropy near the phase boundary is a challenging task. On the other hand, the lattice computation of W_s relies on production rate of strangeness being sufficiently fast, which cannot be expected near to the phase boundary. Moreover, the variable s/S probes all QGP degrees of freedom, while W_s probes only quark degrees of freedom. We thus conclude that s/S is both more accessible theoretically and experimentally, and perhaps more QGP related observable, as compared to W_s , since it comprises the gluon degrees of freedom.

5.4 Strangeness chemical non-equilibrium

In order that in fast hadronization there is continuity of strangeness Eq. (39), and entropy, Eq. (40) the hadron phase $\gamma_s^H \neq 1$ and $\gamma_q^H \neq 1$. We have to solve for γ_s^H and γ_q^H simultaneously Eqs. (39,40).

In figure 6 we show as a function of T the strange phase space occupancy γ_s^H , obtained for several values of s/S ratio (from top to bottom 0.045, 0.04, 0.035, 0.03, 0.025) evaluated for $S^Q = S^H$. The solid line shows γ_q^H for $s^Q = s^H$ and $S^Q = S^H$. The maximum allowed value Eq. (37) is shown dashed (red).

In figure 7 we show results for γ_s^H/γ_q^H (where $\gamma_q^H = 1$ we show γ_s^H). We consider the three cases: $\gamma_q = 1$, $\gamma_q^H = \gamma_q^{cr}$, and entropy conservation $S^H = S^Q$ for $s/S = 0.045$, $s/S = 0.04$, $s/S = 0.035$, $s/S = 0.03$, $s/S = 0.025$ (dash-dot lines) (lines from top to bottom). We see that except in

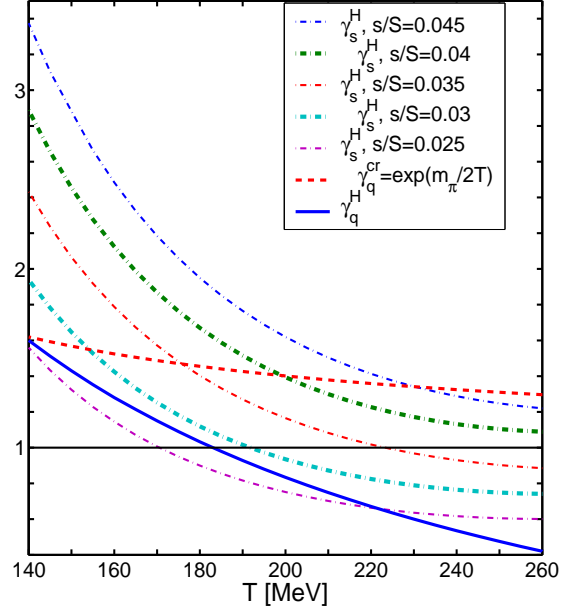


Fig. 6. (color on-line) Phase space occupancy as a function of T : γ_q^H (blue, solid line), γ_s^H (dash-dotted lines, from top to bottom) for $s/S = 0.045$, for $s/S = 0.04$ (thick line), $s/S = 0.035$, $s/S = 0.03$ (thick line), $s/S = 0.025$; γ_q^{cr} (red, dashed line).

case that strangeness were to remain well below chemical equilibrium in QGP ($s/S \simeq 0.03$), the abundance of heavy flavor hadrons we turn to momentarily will be marked by an overabundance of strangeness, since practically in all realistic conditions we find $\gamma_s^H > \gamma_q^H$.

In figure 8 we show s/S ratio as function of γ_s^H/γ_q^H . The solid line is for $T = 200$ MeV, $\gamma_q^H = 0.83$, $S^Q = S^H$, dashed line for $T = 170$ MeV, $\gamma_q^H = 1.15$, $S^Q = S^H$ and dash-dot line for $T = 140$, $\gamma_q^H = 1.6$ MeV, $S^Q = S^H$. We also consider $\gamma_q = 1$ case for $T = 170$ MeV (dot marked (purple) solid line). In this case strangeness content γ_s/γ_q is higher than for $S^H = S^Q$ with the same T and s/S . In the limit $\gamma_q^H = \gamma_q^{cr}$, Eq. 37, ($T = 200$ MeV, solid, thin line; $T = 170$ MeV, dashed line) the strangeness content γ_s^H/γ_q^H is minimal for given T and s/S .

These results suggest that it is possible to measure the value of s/S irrespective of what the hadronization temperature may be, as long as the main yield dependence is on the ratio γ_s^H/γ_q^H . Indeed, we find that the ratio ϕ/K^+ ;

$$\frac{\phi}{K^+} = \frac{\gamma_s^H n_\phi^{eq}}{\gamma_q^H n_{K^+}^{eq}}, \quad (44)$$

is less sensitive to hadronization temperature compared to its strong dependence on the value of s/S . In figure 9 we show the total hadron phase space ratio ϕ/K^+ as function of T for several s/S ratios, and for $\gamma_{s,q}^H = 1$ (chemical equilibrium, dashed (red) line). The K^+ yield contains the contribution from the decay of ϕ into kaons which is a noticeable correction.

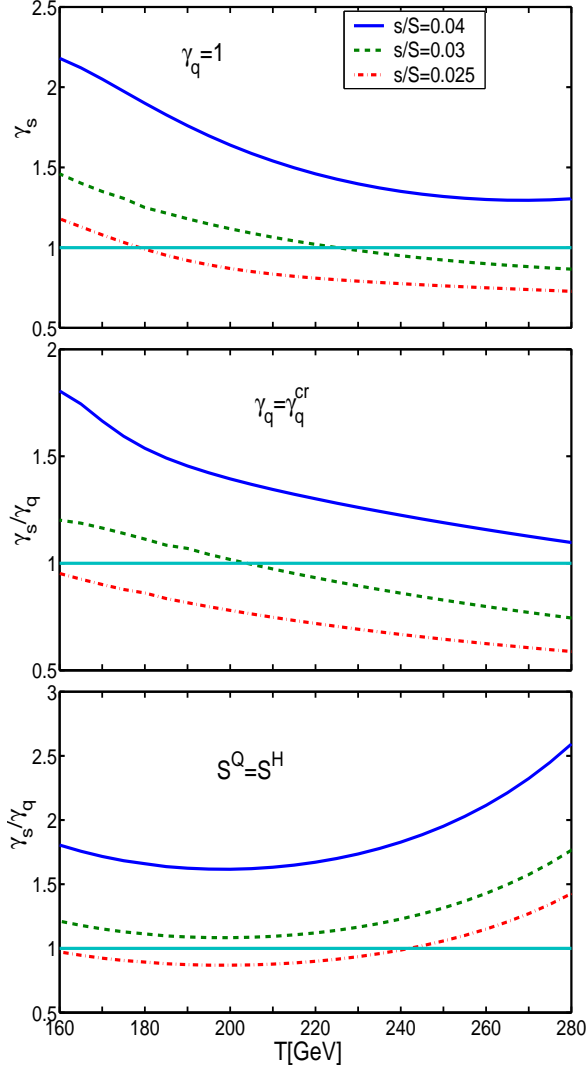


Fig. 7. (color on line) γ_s^H/γ_q^H ($=\gamma_s^H$ at $\gamma_q^H = 1$) as a function of hadronization temperature T . Top frame: $\gamma_q^H = 1$, middle frame: $\gamma_q^H = \gamma_q^{cr}$, and bottom frame: $S^H = S^Q$. Lines, from top to bottom: $s/S = 0.04$ (blue, solid line), $s/S = 0.03$ (green, dashed line), $s/S = 0.025$ (red, dash-dot line)

Table 3. Specific and absolute strangeness yield for different reaction volumes at $T = 200$.

s/S	ds/dy	dV/dy [fm^{-3}]	T [MeV]
0.045	550	1000	200
0.04	360	800	200
0.035	250	700	200
0.03	165	600	200
0.025	106	500	200
0.022	83	500	200

We record in table 3 for given s/S and volume dV/dy the corresponding total yields of strangeness, which may be a useful guide in consideration of the consistency of experimental results with what we find exploring heavy flavor hadron abundance.

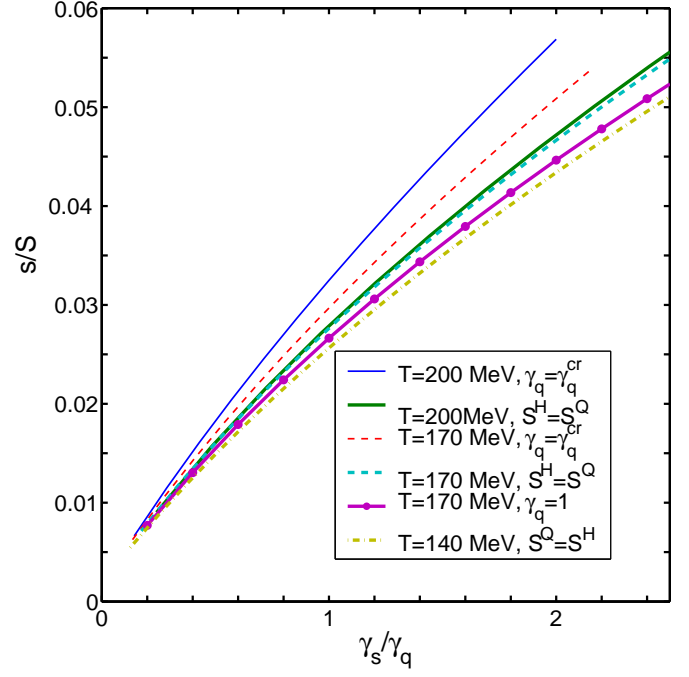


Fig. 8. (color on line) Strangeness to entropy ratio, s/S , as a function of γ_s/γ_q for $T = 200$ MeV, $\gamma_q = 0.083$, $S^H = S^Q$ (solid line), $T = 170$ MeV, $\gamma_q = 1.15$, $S^H = S^Q$ (dashed line), $T = 140$ MeV, $\gamma_q = 1.6$, $S^H = S^Q$ (dash-dotted line); $\gamma_q = 1$ (dot marked solid); $\gamma_q = \gamma_q^{cr}$: $T = 200$ MeV (thin solid line), $T = 170$ MeV (thin dashed line).

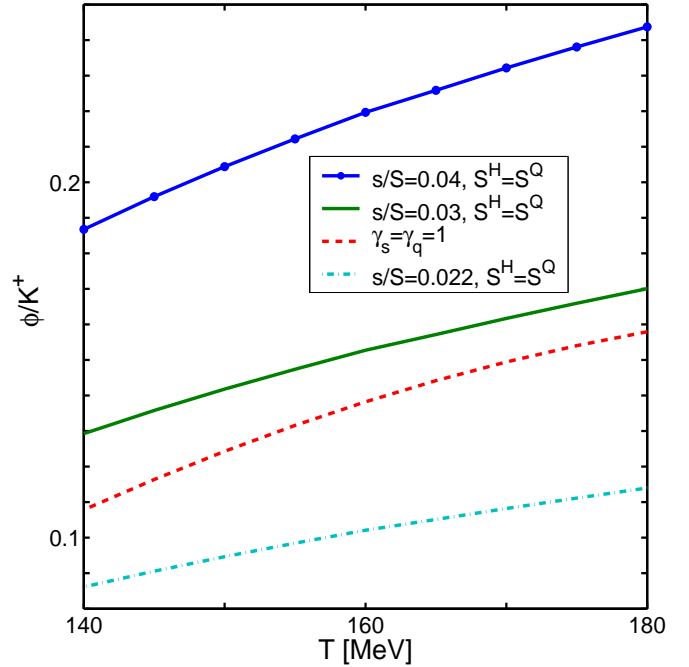


Fig. 9. (Color on line) The ratio ϕ/K^+ as a function of T . Dashed line (red) is for chemical equilibrium. Solid line with dots (green) $s/S = 0.03$, solid line (blue) $s/S = 0.04$, dash-dot line (per) is for $s/S = 0.022$.

6 Yields of heavy flavored hadrons

6.1 Phase space occupancy γ_c^H and γ_b^H

The first step in order to determine the yields of heavy flavor hadronic particles is the determination of the phase space occupancy γ_c^H and γ_b^H . γ_c^H is obtained from equality of number of these quarks (i.e. of quark and anti quark pairs) in QGP and HG. The yield constraint is:

$$\frac{dN_c}{dy} = \frac{dV}{dy} [\gamma_c^H n_{op}^c + \gamma_c^{H2} (n_{hid}^{ceq} + 2\gamma_q^H n_{ccq}^{eq} + 2\gamma_s^H n_{ccs}^{eq})]; \quad (45)$$

where open ‘op’ charm yield is:

$$n_{op}^c = \gamma_q^H n_D^{eq} + \gamma_s^H n_{D_s}^{eq} + \gamma_q^{H2} n_{qqc}^{eq} + \gamma_s^H \gamma_q^H n_{sqc}^{eq} + \gamma_s^{H2} n_{ssc}^{eq}. \quad (46)$$

Here n_D^{eq} and $n_{D_s}^{eq}$ are densities of D and D_s mesons, respectively, in chemical equilibrium, n_{qqc}^{eq} is equilibrium density of baryons with one charm and two light quarks, n_{sqc}^{eq} is density of baryons with one charm (or later on one bottom quark) and two strange quarks (Ω_c^0 , Ω_b^0) in chemical equilibrium and n_{hid}^{eq} is equilibrium particle density with both, a charm (or bottom) and an anticharm (or antibottom) quark ($C=0$, $B=0$, $S=0$). The equilibrium densities can be calculated using Eq.(4). γ_c^H can now be obtained from Eq.(45).

Similar calculations can be done for γ_b^H . The only difference is that we need to add number of B_c mesons to the right hand side of Eq.(45),

$$\frac{dN_{B_c}}{dy} = \gamma_b^H \gamma_c^H n_{B_c}^{eq} \frac{dV}{dy}. \quad (47)$$

$n_{B_c}^{eq}$ is density in chemical equilibrium of B_c . In the calculation of γ_c^H the contribution of term with n_{B_c} is very small and we did not consider it above.

The value of γ_c is in essence controlled by the open single charm mesons and baryons. For this reason we do not consider the effect of exact charm conservation. The relatively small effects due to canonical phase space of charm are leading to a slight up-renormalization of the value of γ_c so that the primary dN_c/dy yield is preserved. This effect enters into the yields of multi-charmed and hidden charm hadrons, where the compensation is not exact and there remains slight change in these yields. However, the error made considering the high yield of charm is not important. On the other hand for multi-bottom and hidden bottom hadrons the canonic effect can be large, depending on actual bottom yield, and thus we will not discuss in this paper yields of these hadrons, pending extension of the methods here developed to include canonical phase space effect.

We consider in figure 10 the temperature dependence of both γ_b^H (top) and γ_c^H (bottom) for the heavy flavor yield given in Eqs. (1,2). In the non-equilibrium case (solid lines) the space occupancy γ_s^H is obtained from Eq.(41) and γ_q^H is chosen to keep $S^H = S^Q$. $\gamma_{c(b)}^H$ depend on γ_s and γ_q : the value of N_s in Eq.(41) is chosen to have $s/S = 0.04$ after hadronization, the corresponding γ_q^H and

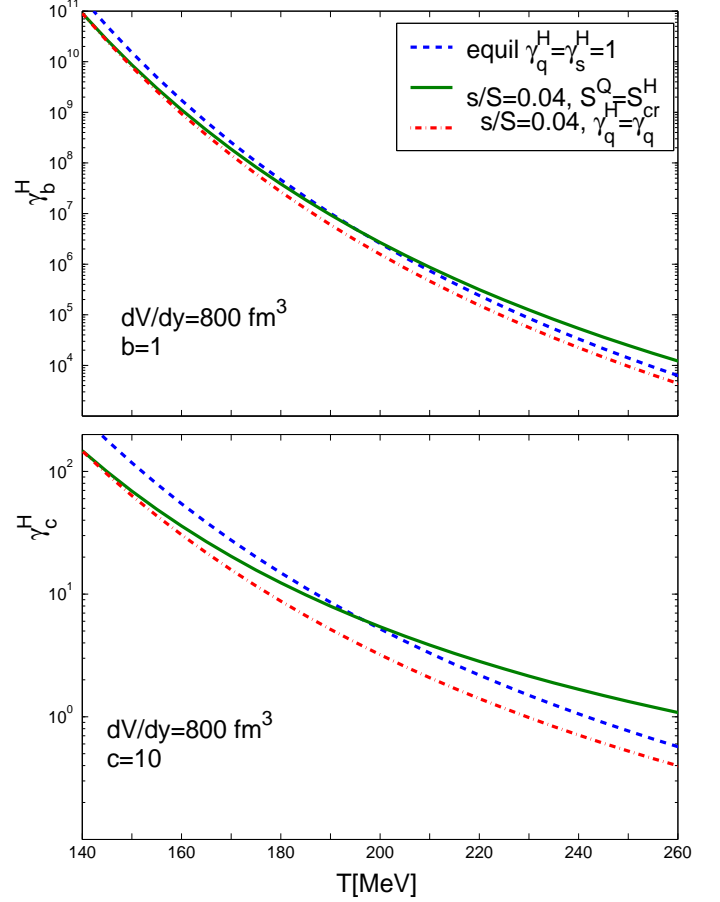


Fig. 10. (Color on line) γ_b^H ($b = 1$) (upper panel), and γ_c^H ($c=10$) (lower panel), as functions of temperature of hadronization T . The solid lines are non-equilibrium for $s/S = 0.04$ with $S^Q = S^H$, dashed lines are equilibrium case $\gamma_s = \gamma_q = 1$ and dot-dash lines are for $s/S = 0.04$ with maximal value of γ_q ($\gamma_q = \gamma_q^{cr}$) ($dV/dy = 800 \text{ fm}^3$).

γ_s^H are shown in figures 6 and 7. Since applicable γ_q^H may depend on hadronization dynamics and/or details of equation of state of QGP, we show charm quark phase space occupancies also for maximum possible value of $\gamma_q^H \rightarrow \gamma_q^{cr}$, also considered at $s/S = 0.04$ for all hadronization temperatures. We can compare our results with the chemical equilibrium (dashed lines) setting $\gamma_s^H = \gamma_q^H = 1$ in Eq.(45). At hadronization condition $T = 160 \pm 20$ MeV temperatures we see in figure 10 a significant (considering the fast changing logarithmic scale) difference between the chemical equilibrium, and non-equilibrium ($s/S=0.04$) results.

In figure 11 we show the ratio $\gamma_{c(b)}^H / \gamma_{c(b)eq}^H$ as a function of hadronization temperature T . This helps us understand when the presence of chemical nonequilibrium is most noticeable. This is especially the case should heavy flavor hadronization occur at the same temperature $T = 140$ – 170 MeV as is obtained for non-heavy hadrons, and/or when the entropy content of light hadrons is maximized with $\gamma_q^H \rightarrow \gamma_q^{cr}$. When no additional entropy is formed

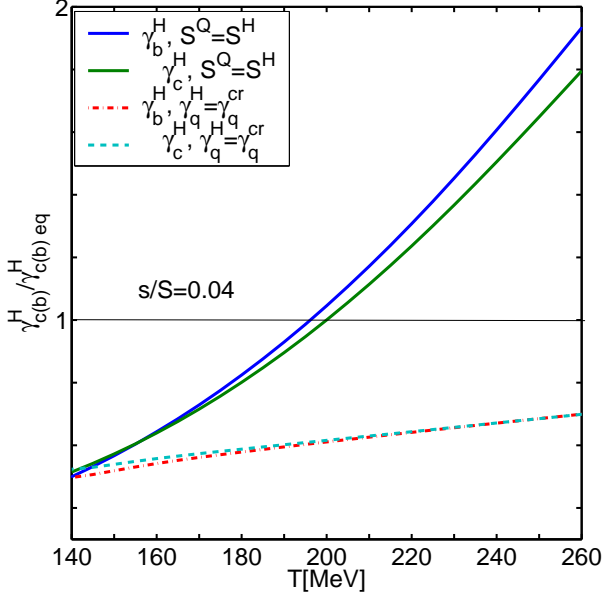


Fig. 11. (Color on line) $\gamma_b^H / \gamma_{b,eq}^H$ and $\gamma_c^H / \gamma_{c,eq}^H$, as functions of temperature of heavy flavor hadronization T . The solid with dot marks line is for $\gamma_b^H / \gamma_{b,eq}^H$ with $s/S = 0.04$, solid line is for γ_c^H with $s/S = 0.04$, dot-dash and dashed lines are for $s/S = 0.04$ with maximal value of $\gamma_q \rightarrow \gamma_q^{cr}$ for $\gamma_b^H / \gamma_{b,eq}^H$ and for $\gamma_c^H / \gamma_{c,eq}^H$, respectively.

in hadronization, that is $S^H = S^Q$, $\gamma_{c(b)}^H / \gamma_{c(b)eq}^H$ exceeds unity for $T > 200$ MeV, at which point the heavy flavor hadron yields exceed the chemical equilibrium expectations. In general we find that heavy hadron yields if produced at normal hadronization temperature would be effectively suppressed, compared to statistical equilibrium results, by the high strangeness yield. This happens since the phase space is bigger at $\gamma_{s,q}^H > 1$, and thus a smaller $\gamma_{c,b}^H$ is required to reach a given heavy flavor yield.

γ_b^H and γ_c^H are nearly proportional to $dN_{b,c}/dy$, respectively. The deviation from the proportionality is due to the abundance of multi-heavy hadrons and it is small. To estimate this effect more quantitatively we first evaluate:

$$\gamma_{c0}^H = \frac{dN_c}{dy} / \left(\frac{dV}{dy} n_{open}^c \right), \quad (48)$$

i.e. the value expected in absence of multi heavy hadrons. Next we compare with the result when we take into account the last three terms in Eq. (45). The influence of these terms depend not only on dN_c/dy but also on $dN_c/dy/dV/dy$. For fixed $dV/dy = 800 \text{ fm}^{-3}$ in the range of $dN_c/dy = (5, 30)$, we find that γ_c^H / N_c (and therefore yields of open charm hadrons) changes at temperature $T = 140$ MeV by $\sim 6\%$ for the $s/S = 0.04$. For the chemical equilibrium case $\gamma_s = \gamma_q = 1$, γ_c^H / N_c changes up to 15% at the same conditions. For the particles with hidden charm or 2 charm quarks the yields are proportional γ_i^2 , therefore changes in their yields will be about twice larger. For RHIC $N_c < 3$ and $dV/dy = 600 \text{ fm}^{-3}$ the dependence of yields on N_c is much smaller.

The multiplicity dN_c/dy can also influence γ_b^H , since as we noted it also includes a term proportional to $\gamma_c^H n_{Bc}^{eq}$. In the range of $N_c = (5, 30)$, γ_b/N_b changes at temperature $T = 0.14$ MeV by $\sim 0.5\%$ for $s/S = 0.04$. Since the mass of b -quark is much larger than that of c -quark, the effect due to multi-bottom states is negligible.

6.2 D, Bs, B, Bs meson yields

In next sections we will mostly consider particles yields after hadronization and we will omit superscript H in γ_s . Considering Eq. (4), we first obtain γ_c as a function of γ_s/γ_q ratio and T . Substituting this γ_c and appropriate equilibrium hadron densities into Eq. (4) we obtain yields of $D(B)$ and $D_s(B_s)$, as functions of the γ_s/γ_q ratio, at fixed temperature, which are shown on figure 12. In the upper panel we show the fractional yields of charmed D/N_c and D_s/N_c mesons, and in the lower panel B/N_b and B_s/N_b for $T = 200$ MeV (solid line), $T = 170$ MeV (dashed line), $T = 140$ MeV (dash-dot line). In general the heavy non-strange mesons yield decreases and strange heavy meson yield increases with γ_s/γ_q . The yields D, B and D_s, B_s are sum over excited states of D, B and D_s, B_s respectively, see table 1 for the ‘vertical tower’ of resonances we have included.

Using $\gamma_c, \gamma_s, \gamma_q$ at a given T (see figures 6, 7, 10) we have now all the inputs required to compute absolute and relative particle yields of all heavy hadrons which we can consider within the grand canonical phase space. When we consider chemical equilibrium case, we use naturally $\gamma_s = \gamma_q = 1$.

In figure 13 we consider the yields shown in figure 12 as a functions of hadronization temperature. The dashed blue and green lines were obtained for chemical equilibrium yields of D and D_s respectively. The extreme upper and lower lines are for fractional D and D_s yields with $s/S = 0.03$ (dot marked, blue and green lines, respectively), while the central lines are for $s/S = 0.04$ (solid, blue and green lines). Also we show fractional yields for maximal possible value $\gamma_q \rightarrow \gamma_q^{cr}$, see figure 6 for $\gamma_q^{cr}(T)$ (dash-dot lines) and Eq. (37).

We note that there is considerable symmetry at fixed T between the fractional yields of charmed, and bottom mesons, for the same condition of s/S . The chemical equilibrium results show significant difference between strange and non-strange heavy mesons. In the case of chemical equilibrium, for the considered very wide range of hadronization temperatures $D_s/N_c \simeq B_s/N_b \simeq 0.2$ are nearly constant. A significant deviation from this result would suggest the presence of chemical non-equilibrium mechanisms of heavy flavor meson production.

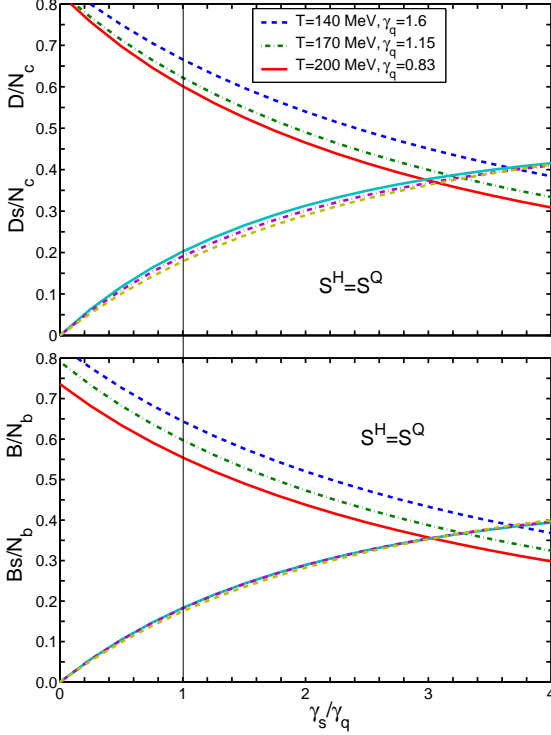


Fig. 12. (Color on line) Upper panel, fractional charm meson yield, and lower panel, fractional bottom meson yields as a function of γ_s/γ_q ratio for fixed hadronization temperature T . Upper lines in each panel are for $D(B)$ mesons, solid line is for $T = 200$ MeV, $\gamma_q = 1.1$, dashed line is for $T = 170$ MeV, $\gamma_q = 1.15$ and dash-dot line is for $T = 140$ MeV, $\gamma_q = 0.83$ ($S^H = S^Q$).

The yields of D_s/N_c and B_s/N_b are very similar, and similarly so for D/N_c and B/N_b . Thus the relative yield of either of these mesons measures the relative yield of charm to bottom participating in the statistical hadronization process:

$$\frac{D_s}{B_s} \simeq \frac{D}{B} = \frac{N_c}{N_b} \quad (49)$$

This is a very precise result, which somewhat depends on the tower of resonances included, and thus in particular on the symmetry in the heavy quark spectra between charmed and bottom states which we imposed.

It is useful to reconsider here the ratio D/D_s (B/B_s) which is proportional to γ_q/γ_s , see figure 1 for D_s/D presented as a function of γ_s/γ_q . We consider this ratio now as a function of T , the upper panel in figure 14 is for charm, the lower for bottom. We see that there is considerable symmetry in the relative yields between charmed and bottom mesons with upper and lower panels looking quasi-identical. Except for accidental values of T where the equilibrium results (blue, dashed lines) cross the fixed s/S results, there is considerable deviation in these ratios expected from chemical equilibrium. For LHC with $s/S = 0.04$ this ratio is always noticeably smaller than in chemical equilibrium (solid purple line is for $S^Q = S^H$ and purple, dash-dot line is for $\gamma_q = \gamma_q^{cr}$). Even for RHIC-

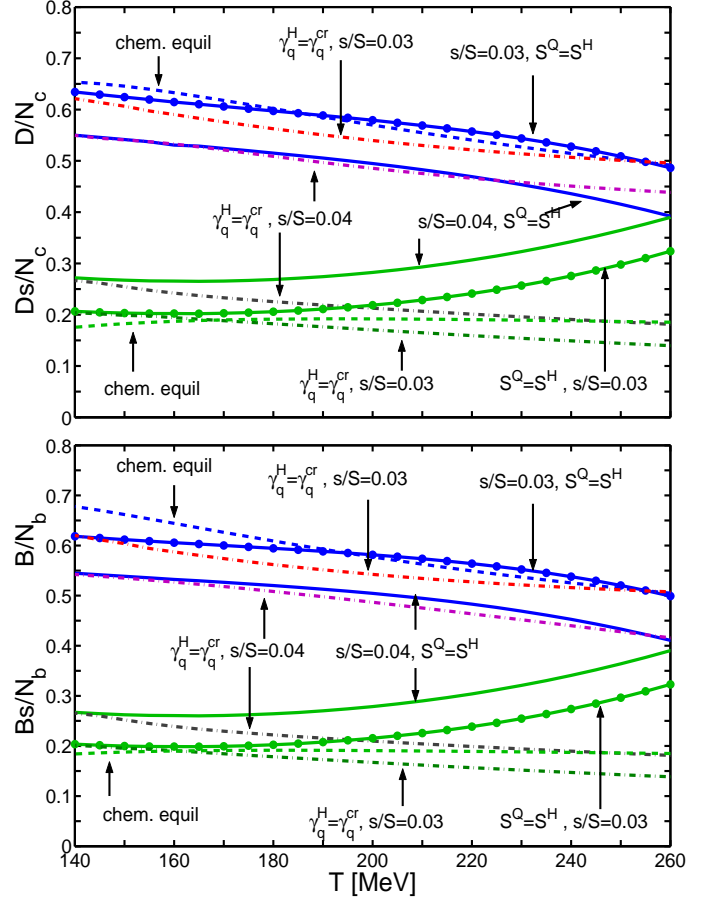


Fig. 13. (Color on line) Upper panel, fractional charm meson yield, and lower panel, fractional bottom meson yields. Equilibrium (dashed lines) and non-equilibrium for $s/S = 0.03$ (point marked solid line) and $s/S = 0.04$ (solid line) for D/N_c (blue lines, upper panel); D_s/N_c (green lines, upper panel); for D/N_c and D_s/N_c with $s/S = 0.03$ and $s/S = 0.04$ for $\gamma_q = \gamma_q^{cr}$ (dash-dotted lines); B/N_b (solid line, lower panel); and B_s/N_b (point marked solid line, lower panel), for B/N_b and B_s/N_b with $s/S = 0.03$ and $s/S = 0.04$ for $\gamma_q = \gamma_q^{cr}$ (dash-dot lines); as a function of T .

like conditions with $s/S = 0.03$ this ratio is smaller than in chemical equilibrium for all temperatures when entropy conservation in hadronization is assumed, $S^Q = S^H$ (dot marked solid, green line).

6.3 Heavy baryon yields

As was the case comparing charm to bottom mesons we also establish a symmetric set of charmed and bottom baryons, shown in the table 4. Many of the bottom baryons are result of theoretical studies and we include that many states to be sure that both charm and bottom are consider in perfect symmetry to each other. In figure 15 (upper panel) we show hadronization temperature dependencies of yields of baryons with one charm quark normalized to charm multiplicity N_c . We show separately yields of baryons without strange quark ($\Lambda_c + \Sigma_c)/N_c$, and with

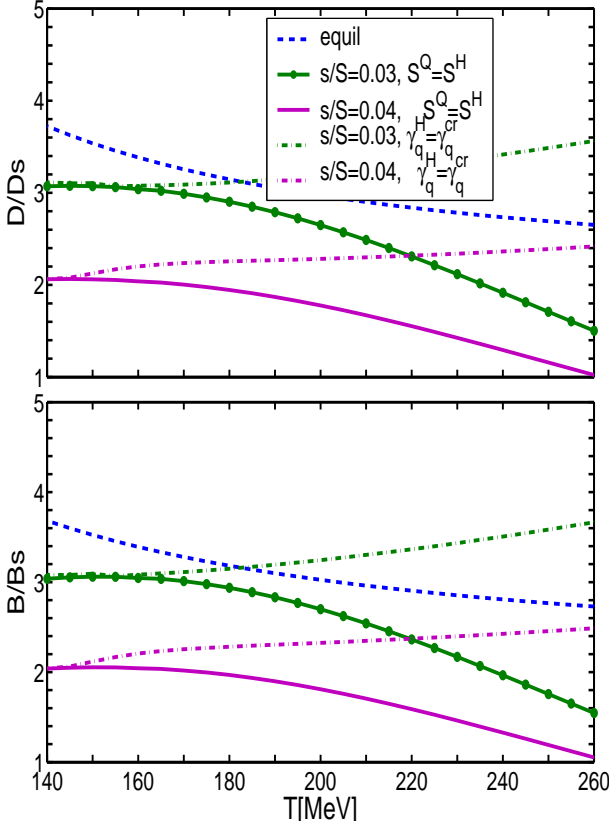


Fig. 14. (Color on line) Ratios D/D_s (upper panel) and B/B_s (lower panel) are shown as a function of T for different s/S ratios and in chemical equilibrium. Solid line is for $s/S = 0.04$, dash-dot line is for $s/S = 0.03$, dashed line is for $\gamma_s^H = \gamma_s^H = 1$.

Table 4. Charm and bottom baryon states considered. States in parenthesis are not known experimentally and have been adopted from theoretical source [31].

hadron	M[GeV]	$Q : c, b$	hadron	M[GeV]	g
$\Lambda_c^+(1/2^+)$	2.285	udQ	$\Lambda_b^0(1/2^+)$	5.624	2
$\Lambda_c^+(1/2^-)$	2.593	udQ	$\Lambda_b^0(1/2^-)$	(6.00)	2
$\Lambda_c^+(3/2^-)$	2.627	udQ	$\Lambda_b^0(1/2^-)$	(6.00)	2
$\Sigma_c^+(1/2^+)$	2.452	qqQ	$\Sigma_b^0(1/2^+)$	(5.77)	6
$\Sigma_c^+(3/2^+)$	2.519	qqQ	$\Sigma_b^0(3/2^+)$	(5.78)	12
$\Xi_c(1/2^+)$	2.470	qsQ	$\Xi_b(1/2^+)$	(5.76)	4
$\Xi_c'(1/2^+)$	2.574	qsQ	$\Xi_b'(1/2^+)$	(5.90)	4
$\Xi_c(3/2^+)$	2.645	qsQ	$\Xi_b'(3/2^+)$	(5.90)	8
$\Omega_c(1/2^+)$	2.700	ssQ	$\Omega_b(1/2^+)$	(6.00)	2
$\Omega_c(3/2^+)$	(2.70)	ssQ	$\Omega_b(3/2^+)$	(6.00)	4

one strange quark $S=1$ (Ξ_c/N_c). We show two cases for $s/S = 0.04$ with conserved entropy at hadronization $S^Q = S^H$ (solid lines) and with maximum possible entropy value $\gamma_q = \gamma_q^{cr}$ (dash-dot lines). The chemical equilibrium case $\gamma_q = \gamma_s = 1$ is also shown (dashed lines). The upper lines of each type are for $(\Lambda_c + \Sigma_c)/N_c$, the lower lines are for Ξ_c/N_c . A similar result is presented for bottom baryons in the lower panel of figure 15. We note that the result for bottom baryons is more uncertain since most baryon masses entering are not experimentally verified.

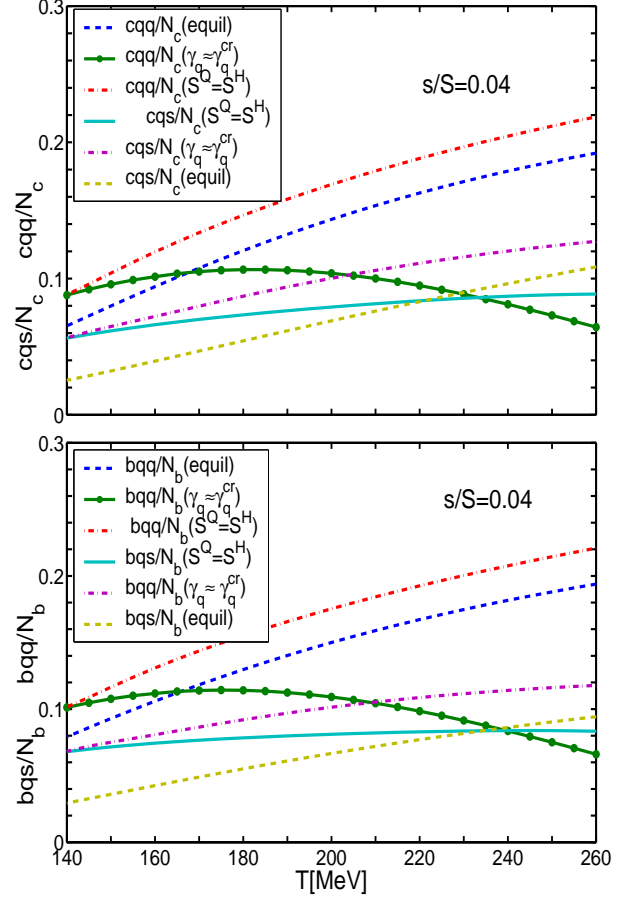


Fig. 15. (Color on line) Equilibrium (dashed lines), $s/S = 0.04$, $S^Q = S^H$ (solid lines), $s/S = 0.04$, $\gamma_q = \gamma_q^{cr}$, (the upper panel) upper lines for each type are for ratio $(\Lambda_c + \Sigma_c)/N_c$ and lower lines are for Ξ_c/N_c (upper panel) and (lower panel) upper lines of each type are for $(\Lambda_b + \Sigma_b)/N_c$ and lower lines are for Ξ_b/N_b as functions of T .

We note that the results shown figure 15 imply that under LHC conditions at least 15% of heavy flavor can be bound in heavy baryons, but possibly 30%. For large $\gamma_q = \gamma_q^{cr} > 1$ we see increase in $(\Lambda_c + \Sigma_c)/N_c$ yields compared to chemical equilibrium and especially compared to entropy conserved hadronization $S^Q = S^H$. This is so since yields are proportional to γ_q^2 , $\gamma_s \gamma_q$. This results to relative suppression the D_s/N_c (see figure 13).

In figure 16 we show ratio $cqq/cqs = (\Lambda_c + \Sigma_c)/\Xi_c$ as a function of γ_s/γ_q for $T = 200$ MeV (dash-dot line), $T = 170$ MeV (solid line) and $T = 140$ MeV (dashed line). This dependence is linear, the slope depends only on hadronization temperature T . The γ_s/γ_q ratio can be converted to s/S ratio using figure 8.

The yield of multi-strange charmed baryon, $\Omega_c(css)$ is, similar to the light multi-strange hadrons, much more sensitive to chemical non-equilibrium. In figure 17 we see a large increase in fractional yield of $\Omega_c(css)/N_c$ for $s/S = 0.04$ and $S^Q = S^H$ (solid line) compared to the chemical equilibrium (dashed line) expectation for the entire considered range of hadronization temperature. As expected,

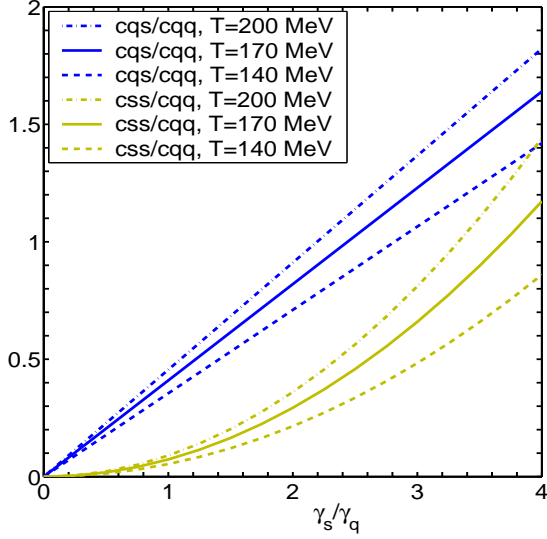


Fig. 16. (Color on line) The ratios $cqs/cqq = \Xi_c/(\Lambda_c + \Sigma_c)$ (upper lines) and $css/cqq = \Omega_c/(\Lambda_c + \Sigma_c)$ (lower lines) for $T = 200\text{MeV}$ (dash-dot line), $T = 170\text{ MeV}$ (solid line) and $T = 140\text{ MeV}$ (dashed line) as functions of γ_s/γ_q .

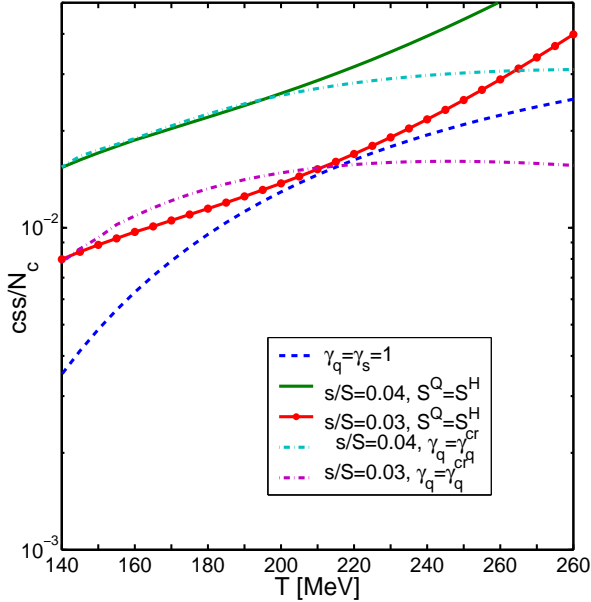


Fig. 17. (Color on line) $\Omega_c(css)/N_c$ as function of T : dashed line for chemical equilibrium; solid lines are for $S^Q = S^H$, dashed dotted lines are for $\gamma_q = \gamma_q^{cr}$: both for $s/S = 0.03$ and $s/S = 0.04$ (upper lines).

this yields increase with T . This also means that higher formation temperature can be invoked to explain an unusually high yield. We expect that at LHC more than one percent of total charm yield will be found in the $\Omega_c(css)$ state.

Table 5. Hidden charm and multi heavy hadron states considered. States in parenthesis are not known experimentally

hadron		mass(GeV)	g
$\eta_c(1S)$	$c\bar{c}$	2.9779	1
$J/\psi(1S)$	$c\bar{c}$	3.0970	3
$\chi_{c0}(1P)$	$c\bar{c}$	3.4152	1
$\chi_{c1}(1P)$	$c\bar{c}$	3.5106	3
$h_c(1P)$	$c\bar{c}$	3.526	3
$\chi_{c2}(1P)$	$c\bar{c}$	3.5563	5
$\eta_c(2S)$	$c\bar{c}$	3.638	1
$\psi(2S)$	$c\bar{c}$	3.686	3
ψ	$c\bar{c}$	3.770	3
$\chi_{c2}(2P)$	$c\bar{c}$	3.929	5
ψ	$c\bar{c}$	4.040	3
ψ	$c\bar{c}$	4.159	3
ψ	$c\bar{c}$	4.415	3
B_c	$b\bar{c}$	6.27	1
Ξ_{cc}	ccq	3.527	4
Ω_{cc}	ccs	(3.660)	2

6.4 Yields of hadrons with two heavy quarks

We consider multi-heavy hadrons listed in the table 5. The yields we will compute are now more model dependent since we cannot completely reduce the result, it either remains dependent on the reaction volume dV/dy , or on the total charm(bottom) yields dN/dy . For example the yields of hadrons with two heavy quarks are approximately proportional to $1/(dV/dy)$ because $\gamma_{b,c}^H$ for heavy quarks is proportional to $1/dV/dy$, see Eq. (45):

$$\frac{dN_{hid}}{dy} \propto \gamma_c^H \frac{dV}{dy} \propto \frac{1}{dV/dy}, \quad (50)$$

$$\frac{dN_{Bc}}{dy} \propto \gamma_c^H \gamma_b^H \frac{dV}{dy} \propto \frac{1}{dV/dy}. \quad (51)$$

Moreover, unlike it is the case for single heavy hadrons, the canonical correction to grand-canonical phase space does not cancel out in these states, adding to the uncertainty.

Thus the result we present must seen as a guiding the eye and demonstrating a principle. In figure 18 we show the yield of hidden charm $c\bar{c}$ mesons (see table 5) normalized by the square of charm multiplicity N_c^2 as a function of hadronization temperature T . We consider again cases with $s/S = 0.03$ (upper panel) and $s/S = 0.04$ (lower panel), solid line is for $S^H = S^Q$, dot-dash line is for $\gamma_q = \gamma_q^{cr}$, and dot-dash line is for $\gamma_q = \gamma_q^{cr}$. The chemical equilibrium $c\bar{c}$ mesons yields are shown (dashed lines on both panels) for two different values of $dV/dy = 600\text{ fm}^3$ for $T = 200\text{ MeV}$ (upper panel) and $dV/dy = 800\text{ fm}^3$ for $T = 200\text{ MeV}$ (lower panel).

The yield of $c\bar{c}$ mesons is much smaller for $s/S = 0.04$ than in equilibrium for the same dV/dy for large range of hadronization temperatures. For $s/S = 0.03$ the effect is similar, but suppression is not as pronounced. For $\gamma_q = \gamma_q^{cr}$ suppression the yield of hidden charm particles is always smaller than equilibrium value. This suppression occurs due to competition with the yield of strange-heavy

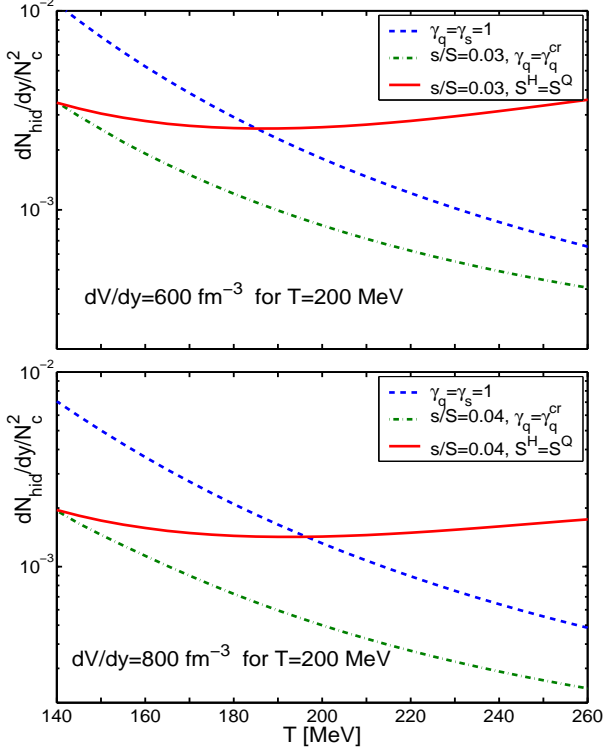


Fig. 18. (Color on line) $c\bar{c}/N_c^2$ yields as a function of hadronization temperature T , at $dV/dy = 600 \text{ fm}^{-3}$ for $T = 200 \text{ MeV}$, $s/S = 0.03$ (upper panel), $dV/dy = 800 \text{ fm}^{-3}$ for $T = 200 \text{ MeV}$, $s/S = 0.04$ (lower panel). Results shown are for $S^Q = S^H$ (solid lines), for $\gamma_q = \gamma_q^{cr}$ (dash-dot lines), and for chemical equilibrium case (dashed lines, s/S is not fixed).

mesons, and also, when $\gamma_q > 1$, with heavy baryons with two light quarks. The enhanced yield of D, D_s and heavy baryons in effect depletes the pool of available charmed quark pairs, and fewer hidden charm $c\bar{c}$ mesons are formed. For particles with two heavy quarks the effect is larger than for hadrons with one heavy quark and light quark(s).

In figure 19 we compare the J/Ψ yield to the chemical equilibrium yield $\Psi/J\Psi_{eq}$, as a function of γ_s^H/γ_q^H , each line is at a fixed value γ_q^H . This ratio is:

$$\frac{J/\Psi}{J\Psi_{eq}} = \frac{N_{hid}}{N_{hid eq}} = \frac{\gamma_c^2}{\gamma_{c eq}^2}. \quad (52)$$

$J/\Psi/J\Psi_{eq}$ always decreases when γ_s/γ_q increases. For $\gamma_q = \gamma_{cr}$ $J/\Psi/J\Psi_{eq}$ is smaller than unity even when $\gamma_s \rightarrow 0$, because of large phase space occupancy of light quarks. $J/\Psi/J\Psi_{eq} > 1$ for small γ_q and small γ_s/γ_q .

Considering the product of J/Ψ and ϕ yields normalized by N_c^2 we eliminate nearly all the uncertainty about the yield of charm and/or hadronization volume. However, we tacitly assume that both J/Ψ and ϕ hadronize at the same temperature. In figure 20 we show $J/\Psi\phi/N_c^2$ as function of γ_s/γ_q . There is considerable difference to the ratio considered in figure 2. We see mainly dependence on γ_s/γ_q . As before, see section 3.2 J/Ψ is the sum of all states $c\bar{c}$ from table 5 that can decay to J/Ψ . We show results for

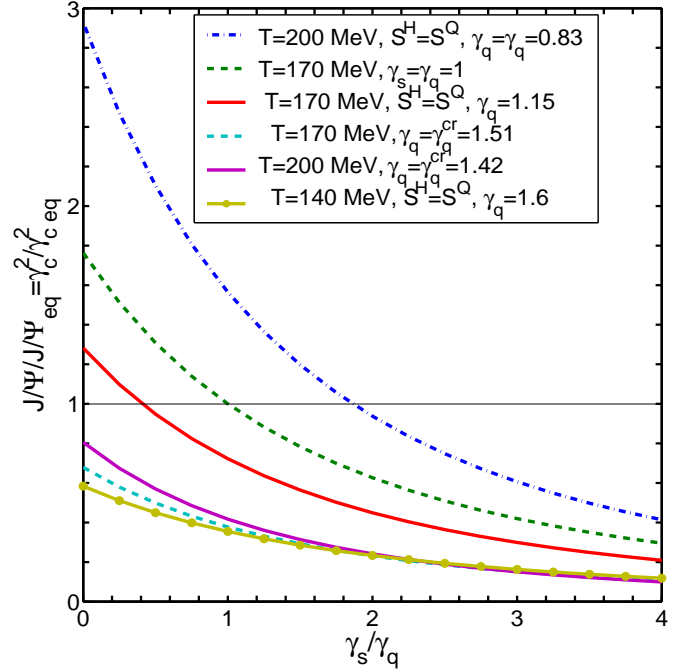


Fig. 19. (Color on line) Ratio $J/\Psi/J\Psi_{eq} = \gamma_c^2/\gamma_{c eq}^2$ as a function of γ_s^H/γ_q^H at fixed value of γ_q^H and if required, entropy conservation. Shown are: $T = 200 \text{ MeV}$ at $\gamma_q = 0.83$ (dot-dash line) and at $\gamma_q = \gamma_q^{cr} = 1.42$ (lower solid line (purple)); $T = 170 \text{ MeV}$ at $\gamma_q = 1$ (upper dashed line), at $\gamma_q = 1.15$, (upper solid line (red)), and at $\gamma_q = \gamma_q^{cr} = 1.51$, (lower dashed line); and $T = 140 \text{ MeV}$, $\gamma_q = 1.6$

$T = 200 \text{ MeV}$ (solid lines), $T = 170 \text{ MeV}$ (dashed line) and $T = 140 \text{ MeV}$ (dash-dot line). The γ_q , for each T , is fixed by entropy conservation condition during hadronization (figure 6) (thick lines) or by $\gamma_q = \gamma_q^{cr}$ (thin lines). For $T = 140 \text{ MeV}$ these lines coincide. $T = 170 \text{ MeV}$, $\gamma_q = 1$ case is also shown (solid line with dot markers). The s/S values, which correspond to given γ_s/γ_q ratio can be found in figure 8. Figure 20 shows that despite the yield $\phi/(dV/dy)$ increasing as $(\gamma_s/\gamma_q)^2$, $J/\Psi\phi/N_c^2$ is increasing as γ_s/γ_q considering compensation effects.

A similar situation, as in figure 19 for hidden charm, arises for the B_c meson yield, see figure 21, where $B_c/N_c N_b$ ratio is shown as a function of hadronization temperature T , for the same strangeness yield cases as discussed for the hidden charm meson yield. Despite suppression in strangeness rich environment, the B_c meson yield continues to be larger than the yield of B_c produced in single NN collisions, where the scale yield is at the level of $\sim 10^{-5}$, see cross sections for $b\bar{b}$ and B_c production in [11] and in [32], respectively.

In figure 22 we show N_c^2 scaled yields of ccq and ccs baryons as a function of temperature. Upper panel shows aside of the equilibrium case (dashed lines) the yields for $s/S = 0.04$ with $S^H = S^Q$ (solid lines) and with $\gamma_q = \gamma_q^{cr}$ (dash-dot line) for $dV/dy = 800 \text{ fm}^{-3}$ for $T = 200 \text{ MeV}$. Lower panel is for $dV/dy = 600 \text{ fm}^{-3}$ and $s/S = 0.03$. For the ccq baryons the chemical non-equilibrium suppression effect is similar to what we saw for $c\bar{c}$ and B_c mesons.

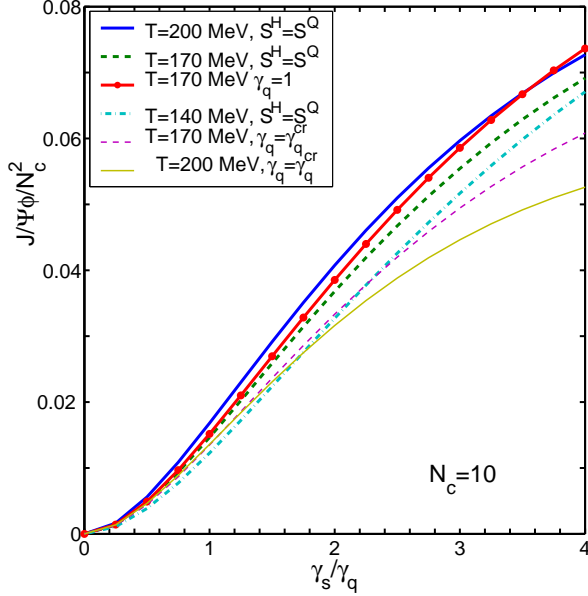


Fig. 20. (Color on line) $J/\Psi\phi/N_c^2$ states yields as a function of γ_s/γ_q ratio for $T = 200$ MeV, $S^H = S^Q$ (solid line) and $\gamma_q = \gamma_q^{cr}$ (solid thin line), $T = 170$ MeV: $S^Q = S^H$ (dashed line), $\gamma_q = \gamma_q^{cr}$ (thin dashed line) and $\gamma_q = 1$ (solid line with dot marker); for $T = 140$ MeV, $S^Q = S^H$ (dash-dot line)

Equilibrium yield is much larger than non-equilibrium for $T < 230$ MeV when $s/S = 0.04$ and $S^H = S^Q$, and for $T < 190$ MeV when $s/S = 0.03$ and $S^H = S^Q$. In case $\gamma_q = \gamma_q^{cr}$, the yield of ccq is always smaller than equilibrium. The yield of ccs baryons has similar suppression, but it becomes larger than equilibrium for smaller temperatures and yield enhancement for higher T is larger for $S^H = S^Q$ then in case of ccq because of large number of strange quarks.

In the figure 23 we show ratios $ccq/J/\Psi$ (upper panel) and $ccs/J/\Psi$ (lower panel) as a function of hadronization temperature. These ratios do not depend on dV/dy . $ccq/J/\Psi \propto \gamma_q$ does not depend on s/S . For $ccq/J/\Psi$ ratio we show three cases: chemical equilibrium $\gamma_s = \gamma_q = 1$ (dashed line), $S^H = S^Q$ (solid line) and $\gamma_q = \gamma_q^{cr}$ (dash-dot line). For $ccs/J/\Psi$ ($ccq/J/\Psi \propto \gamma_s$) we show chemical equilibrium case (dashed line), $s/S = 0.04$: $S^H = S^Q$ (solid line with point marker) and $\gamma_q = \gamma_q^{cr}$ (thin dash-dot line); $s/S = 0.03$: $S^H = S^Q$ (solid line) and $\gamma_q = \gamma_q^{cr}$ (thin dash-dot line). The overall all yields of double charmed (strange and non-strange) baryons and anti-baryons is clearly larger than the yield of J/Ψ .

7 Conclusions

We have considered here in some detail the abundances of heavy flavor hadrons within the statistical hadronization model. While we compare the yields to the expectations based on chemical equilibrium yields of light and strange quark pairs, we present results based on the hypothesis that the QGP entropy and QGP flavor yields determine

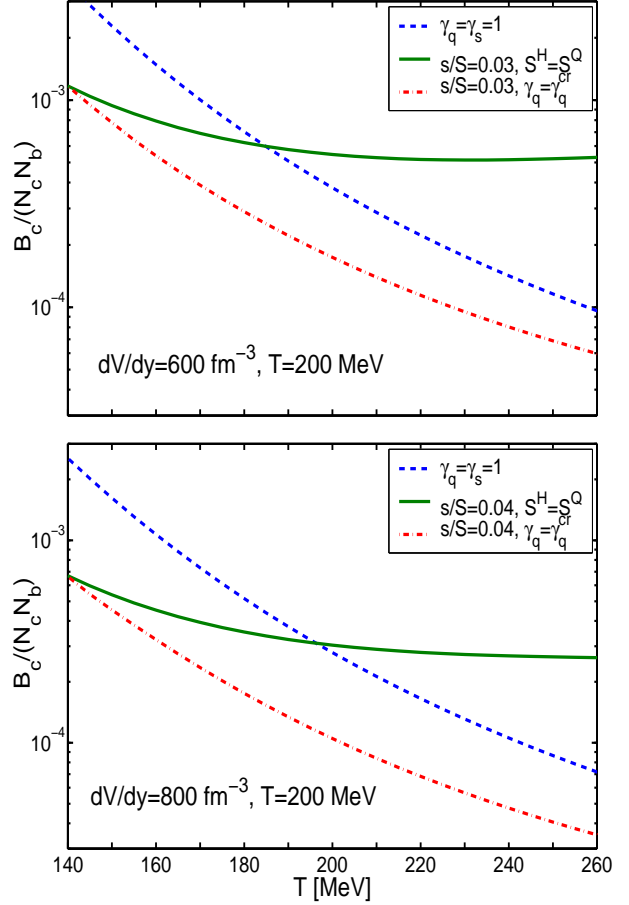


Fig. 21. (Color on line) B_c mesons yields as function of T for chemical equilibrium case with $dV/dy = 600 \text{ fm}^{-3}$ for $T = 200$ MeV (the upper panel, dashed line), for $s/S = 0.03$ with $dV/dy = 600 \text{ fm}^{-3}$ for $T = 200$ MeV (the upper panel, solid line), for chemical equilibrium case with $dV/dy = 800 \text{ fm}^{-3}$ for $T = 200$ MeV (the lower panel, dashed line) for $s/S = 0.04$ $dV/dy = 800 \text{ fm}^{-3}$ for $T = 200$ MeV (lower panel, solid line)

the values of phase space occupancy γ_i^H $i = q, s, c, b$, which are of direct interest in study of the heavy hadron yields.

For highest energy heavy ion collisions the range of values discussed in literature is $1 \leq \gamma_q^H \leq 1.65$ and $0.7 \leq \gamma_s^H/\gamma_q^H \leq 1.5$. However γ_c^H and γ_b^H values which are much larger than unity arise. This is due to the need to describe the large primary parton based production, and considering that the chemical equilibrium yields are suppressed by the factor $\exp(-m/T)$.

Our work is based on the grand canonical treatment of phase space. This approach is valid for charm hadron production at LHC, since the canonical corrections, as we have discussed, are not material. On the other hand, even at LHC the much smaller yields of bottom heavy hadrons are subject to canonical suppression. The value of the parameter γ_b^H obtained at a fixed bottom yield N_b , using either the canonical, or the grand canonical methods, are different, see e.g. Eq. (15) in [33]. Namely, to obtain a given yield N_b in canonical approach, a greater value of γ_b^H is needed in order to compensate the canonical suppression

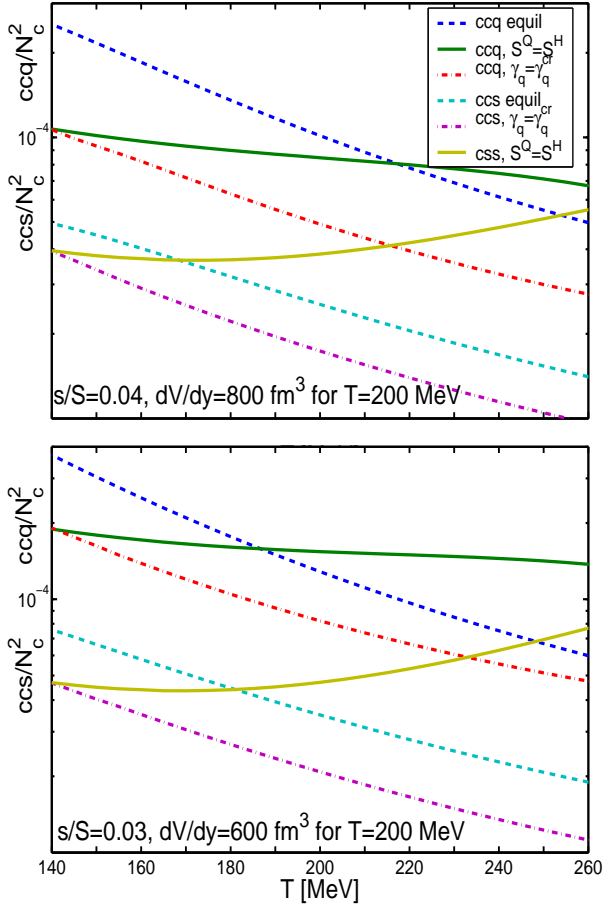


Fig. 22. (Color on line) ccq/N_c^2 (upper lines in each panel) and ccs/N_c^2 (lower lines in each panel) baryon yields as a function of T . Upper panel: chemical equilibrium case with $dV/dy = 800 \text{ fm}^{-3}$ for $T = 200 \text{ MeV}$ (dashed line), $s/S = 0.04$ with $dV/dy = 800 \text{ fm}^{-3}$ for $T = 200 \text{ MeV}$: $S^H = S^Q$ (solid line) and $\gamma_q = \gamma_q^{cr}$ (dash-dot line); and lower panel: chemical equilibrium case with $dV/dy = 600 \text{ fm}^{-3}$ for $T = 200 \text{ MeV}$ (dashed line), and $s/S = 0.03$ $S^Q = S^H$ (solid line) and $\gamma^q = \gamma_q^{cr}$ (dash-dot line).

effect. However, for any individual single- b hadron, the relative yields, i.g. B/B_s do not depend on γ_b^H and thus such ratios are not influenced by canonical suppression. Moreover, as long as the yield of single- b hadrons dominates the total bottom yield: $N_b \simeq B + B_s + \Lambda_b + \dots$, also the N_b scaled yields of hadrons comprising one b -quark i.e. ratios such as B/N_b , B_s/N_b , B_c/N_b , etc, are not sensitive to the value of γ_b^H and can be obtained within either the canonical, or grand canonical method. On the other hand for $b\bar{b}$ mesons and multi- b baryons the canonical effects should be considered. Study of the yields of these particles is thus postponed.

We address here in particular how the yields of heavy hadrons are influenced by $\gamma_s^H/\gamma_q^H \neq 1$ and $\gamma_q \neq 1$. The actual values of γ_s^H/γ_q^H we use are related to the strangeness per entropy yield s/S established in the QGP phase. Because the final value s/S is established well before hadronization, and the properties of the hadron phase space are well understood, the resulting γ_s^H/γ_q^H are well defined and turn

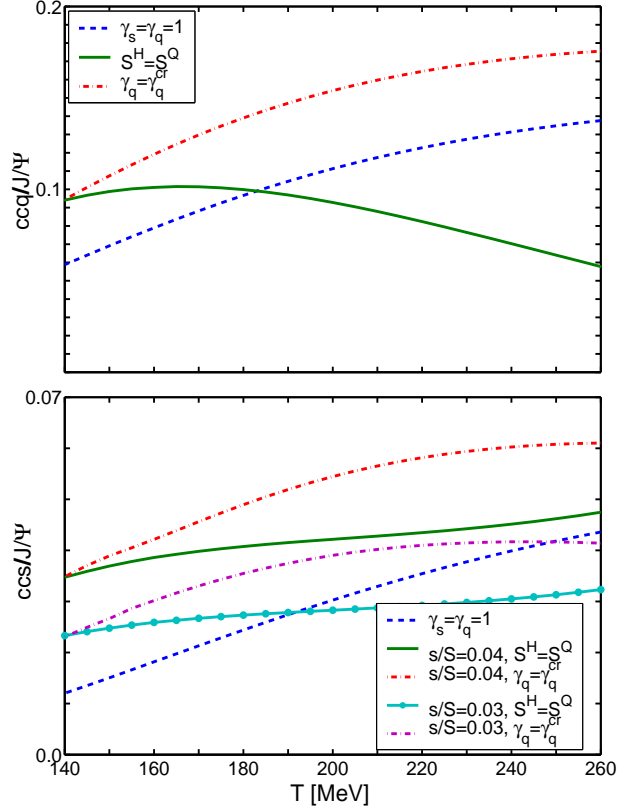


Fig. 23. (Color on line) $ccq/J/\Psi$ (upper panel) and $ccs/J/\Psi$ (lower panel) ratios as a function of T . Upper panel: chemical equilibrium case (dashed line), $S^H = S^Q$ (solid line) and $\gamma_q = \gamma_q^{cr}$ (dashed-dot line); and lower panel: chemical equilibrium case with (dashed line), $s/S = 0.04$: $S^Q = S^H$ (solid line with dot marker) and $\gamma_q = \gamma_q^{cr}$ (thin dash-dot line); $s/S = 0.03$ (solid line) and $\gamma_q = \gamma_q^{cr}$ (thin dash-dot line).

out to be quite different from unity in the range of temperatures in which we expect particle freeze-out to occur. We consider in some detail the effect of QGP hadronization on the values of γ_s^H and γ_q^H .

One of first results we present (figure 2) allows a test of the statistical hadronization model for heavy flavor: we show that the yield ratio $c\bar{c} s\bar{s}/(c\bar{s} \bar{c}s)$ is nearly independent of temperature and it is also nearly constant when the ϕ is allowed to freeze-out later (figure 3), provided that the condition of production is at the same value of strangeness per entropy s/S .

We studied in depth how the (relative) yields of strange and non-strange charmed mesons vary with strangeness content. For a chemically equilibrated QGP source, there is considerable shift of the yield from non-strange D to the strange D_s for $s/S = 0.04$ expected at LHC. The expected fractional yield $D_s/N_c \simeq B_s/N_b \simeq 0.2$ when one assumes $\gamma_s^H = \gamma_q^H = 1$, the expected enhancement of the strange heavy mesons is at the level of 30% when $s/S = 0.04$, and greater when greater strangeness yield is available.

A consequence of this result is that we find a relative suppression of the multi-heavy hadrons, except when they contain strangeness. The somewhat ironic situation

is that while higher beyond chemical equilibrium charm QGP yield enhances production of $c\bar{c}$ states, beyond chemical equilibrium enhanced light quarks and strangeness multiplicity suppresses this almost by that much. This new phenomenon adds to the complexity of interpretation of hidden charm meson yield. On the other hand, the yield of $c\bar{c}/N_c^2 \simeq 210^{-3}$ is found to be almost independent on hadronization temperature in case which conserves entropy at hadronization. We don't know exactly equation of state in QGP and so the value of γ_q which is needed to conserve the entropy may be different. If γ_q is larger for higher temperatures, suppression of $c\bar{c}$ is larger for a fixed s/S . The same result is found for $B_c \approx 5 - 6 \cdot 10^{-4} N_c N_b$, that yield remains considerably larger (by a factor 10 — 100) compared to the scaled yield in single nucleon nucleon collisions.

We have shown that the study of heavy flavor hadrons will provide important information about the nature and properties of the QGP hadronization. The yield of $B_c(b\bar{c})$ mesons remains enhanced while the hidden charm $c\bar{c}$ states encounter another suppression mechanism, compensating for the greatly enhanced production due to large charm yield at LHC.

Acknowledgments

Work supported by a grant from: the U.S. Department of Energy DE-FG02-04ER4131.

References

1. K. Geiger, Phys. Rev. D **48**, 4129 (1993).
2. M. Cacciari, P. Nason and R. Vogt, Phys. Rev. Lett. **95**, 122001 (2005) [arXiv:hep-ph/0502203].
3. H. van Hees and R. Rapp, Phys. Rev. C **71**, 034907 (2005) [arXiv:nucl-th/0412015].
4. M. Schroedter, R. L. Thews and J. Rafelski, Phys. Rev. C **62**, 024905 (2000) [arXiv:hep-ph/0004041].
5. F. Becattini, Phys. Rev. Lett. **95**, 022301 (2005) [arXiv:hep-ph/0503239].
6. R. L. Thews, Eur. Phys. J. C **43**, 97 (2005) [arXiv:hep-ph/0504226].
7. I. Kuznetsova and J. Rafelski, J. Phys. G **32**, S499 (2006) [arXiv:hep-ph/0605307].
8. P. Koch, B. Muller and J. Rafelski, Phys. Rept. **142**, 167 (1986).
9. A. Andronic, P. Braun-Munzinger, K. Redlich and J. Stachel, Phys. Lett. B **571**, 36 (2003) [arXiv:nucl-th/0303036].
10. M. Bedjidian *et al.*, "Hard probes in heavy ion collisions at the LHC: Heavy flavour physics," arXiv:hep-ph/0311048, in: M. Mangano, H. Satz and U. Wiedermann, "Hard probes in heavy-ion collisions at the LHC," pp247-346, CERN-2004-009, Yellow Report, <http://doc.cern.ch/cernrep/2004/2004-009/2004-009.html>
11. K. Anikeev *et al.*, "B physics at the Tevatron: Run II and beyond," arXiv:hep-ph/0201071, SLAC-REPRINT-2001-056, FERMILAB-PUB-01-197, Dec 2001. 583pp. *Workshop on B Physics at the Tevatron: Run II and Beyond, Batavia, Illinois, 24-26 Feb 2000.*
12. J. Letessier and J. Rafelski, Phys. Rev. C **75**, 014905 (2007) [arXiv:nucl-th/0602047].
13. E. Fermi, Prog. Theor. Phys. **5**, 570 (1950).
14. R. Hagedorn, "How We Got To QCD Matter From The Hadron Side By Trial And Error," CERN-TH-3918/84 *Invited talk given at Quark Matter 1984, 4th Int. Conf. on Ultrarelativistic Nucleus-Nucleus Collisions, Helsinki, Finland, Jun 17-21, 1984* K. Kajantie, ed. Springer-Verlag, Lecture Notes in Physics, 221, pp53-76.
15. E. Cheu [the D0 collaboration], Int. J. Mod. Phys. A **20**, 3664 (2005).
16. J. D. Bjorken, Phys. Rev. D **27**, 140 (1983).
17. J. I. Kapusta, Nucl. Phys. B **148**, 461 (1979).
18. S. Hamieh, J. Letessier and J. Rafelski, Phys. Rev. C **62** (2000) 064901 [arXiv:hep-ph/0006085].
19. Joseph I. Kapusta, and Charles Gale, *Finite-Temperature Field Theory : Principles and Applications* Cambridge Monographs on Mathematical Physics, 2006, ISBN: 0521820820
20. J. Letessier and J. Rafelski, Phys. Rev. C **67**, 031902 (2003) [arXiv:hep-ph/0301099]; J. Rafelski and J. Letessier, Nucl. Phys. A **702**, 304 (2002) [arXiv:hep-ph/0112027].
21. G. Torrieri, S. Steinke, W. Broniowski, W. Florkowski, J. Letessier and J. Rafelski, (SHARE 1) Comput. Phys. Commun. **167**, 229 (2005) [arXiv:nucl-th/0404083]; G. Torrieri, S. Jeon, J. Letessier and J. Rafelski, (SHARE 2) Comput. Phys. Commun. **175**, 635 (2006) [arXiv:nucl-th/0603026].
22. J. Letessier, A. Tounsi, U. W. Heinz, J. Sollfrank and J. Rafelski, Phys. Rev. Lett. **70**, 3530 (1993) [arXiv:hep-ph/9711349].
23. J. Letessier, A. Tounsi, U. W. Heinz, J. Sollfrank and J. Rafelski, Phys. Rev. D **51**, 3408 (1995) [arXiv:hep-ph/9212210].
24. J. I. Kapusta and A. Mekjian, Phys. Rev. D **33** (1986) 1304.
25. J. Letessier, J. Rafelski and A. Tounsi, Phys. Lett. B **323**, 393 (1994) [arXiv:hep-ph/9711345].
26. A. Wroblewski, Acta Phys. Polon. B **16**, 379 (1985).
27. R. V. Gavai and S. Gupta, Phys. Rev. D **65**, 094515 (2002) [arXiv:hep-lat/0202006].
28. R. V. Gavai and S. Gupta, J. Phys. G **32**, S275 (2006) [arXiv:hep-ph/0605254]; R. V. Gavai and S. Gupta, Eur. Phys. J. C **43**, 31 (2005) [arXiv:hep-ph/0502198].
29. J. Rafelski and J. Letessier, Eur. Phys. J. A **29** (2006) 107 [arXiv:nucl-th/0511016].
30. T. Matsuki and T. Morii, Phys. Rev. D **56**, 5646 (1997) [Austral. J. Phys. **50**, 163 (1997)] [arXiv:hep-ph/9702366].
31. C. Albertus, J. E. Amaro, E. Hernandez and J. Nieves, Nucl. Phys. A **740**, 333 (2004) [arXiv:nucl-th/0311100].
32. C. H. Chang and X. G. Wu, Eur. Phys. J. C **38**, 267 (2004) [arXiv:hep-ph/0309121].
33. J. Rafelski and J. Letessier, J. Phys. G **28**, 1819 (2002) [arXiv:hep-ph/0112151].